Deterministic Down-Converter and Continuous Photon-Pair Source within the Bad-Cavity Limit

Yue Chang,[1] Alejandro González-Tudela,[1] Carlos Sánchez Muñoz,[1,2] Carlos Navarrete-Benlloch,[1,3] and Tao Shi[1]
[1]*Max-Planck Institut für Quantenoptik, Hans-Kopfermann-Strasse 1, D-85748 Garching, Germany*
[2]*Física Teórica de la Materia Condensada, Universidad Autónoma de Madrid, 28049 Madrid, Spain*
[3]*Institute for Theoretical Physics II, Universität Erlangen-Nürnberg, Staudtstrasse 7, 91058 Erlangen, Germany*
(Received 2 December 2015; revised manuscript received 18 August 2016; published 10 November 2016)

The development, characterization, and control of N-photon sources are instrumental for quantum technological applications. This work constitutes a step forward in this direction, where we propose a cavity quantum electrodynamics setup designed for the generation of photon pairs. We identify both the regime where our system works as a deterministic down-converter of a single input photon and as an optimal two-photon source under weak continuous driving. We use both the scattering and master equation formalisms to characterize the system, and from their connection naturally arises a physical criterion characterizing when weakly driven systems behave as continuous antibunched two-photon sources. We also show that the outgoing photons share nontrivial quantum correlations in general. We provide a specific implementation based on state-of-the-art superconducting circuits, showing how our proposal is within the reach of current technologies. As an outlook, we show the proposal can be extended to achieve deterministic conversion of a single photon into N photons.

DOI: 10.1103/PhysRevLett.117.203602

Single-photon sources [1] are one of the cornerstones of many quantum information protocols [2,3]. The success in the fabrication of these sources is built upon the simple nonlinear systems required, e.g., a two-level system [4], and a well-established characterization through the well-known second-order coherence function [5] $g^{(2)}(\tau)$ (see definition below), which yields $g^{(2)}(0) = 0$ for a perfect single-photon source. The extension to N-photon sources lies also at the heart of many recent quantum technological applications such as the generation of NOON states [6] instrumental for quantum metrology [7], beating the diffraction limit [8], or even biological purposes [9,10]. There exist several methods to generate multiphoton states, e.g., probabilistic schemes using down-converted photons [11] and postselection [12–14], but at the price of an exponentially small probability. An alternative consists in using atomlike systems strongly coupled to cavities [15] or biexciton states in quantum dots systems [16–18]. The former has shown spectacular advances in the microwave regime for intracavity fields [19,20], but its extension to traveling photons is so far limited to single photons [21–24]. Therefore, the efficient generation of multiphoton states is still a challenge which attracts a lot of attention, with new theoretical proposals that use Purcell enhancement on dressed atomic systems [25,26] or atomic ensembles in waveguide QED [27]. Moreover, the question on how to characterize continuous multiphoton sources in a more economical way than performing full-state tomography, is still open, with many different definitions in the literature [25,26,28–31].

In this Letter, we introduce a cavity quantum electrodynamics setup that deterministically converts a single photon into an entangled two-photon state and does so within the *bad-cavity limit*, that is, without requiring coherent interactions to be stronger than cavity or emitter damping. We also analyze the regime when the system is weakly driven and show that the condition for deterministic down-conversion also leads to an optimal continuous source of photon pairs. From the connection between these two regimes, we also propose a general criterion that characterizes when such weakly driven systems behave as emitters of photon pairs in well-defined pulses. Finally, we discuss possible implementations focusing on currently available circuit QED architectures and comment on the possibility to generalize our results for the generation of N-photon states.

Let us first consider the general scheme for a source depicted in Fig. 1(a). A nonlinear system S is coupled to two (one-dimensional) baths [32]. The *pump* bath is used to excite the system with, e.g., a continuous driving or pulses with well-defined photon number, while the emitted light is monitored through the *signal* bath. Working in a picture rotating at some characteristic frequency of the system k_p that we will choose later (using $\hbar = c = 1$), and denoting by $\{p_k, s_k\}_{k\in\mathbb{R}}$ the annihilation operators of the baths, the Hamiltonian is given by $H = H_S + H_B + H_{SB}$, with Hamiltonians H_S and $H_B = \int dk k(p_k^\dagger p_k + s_k^\dagger s_k)$ for system and bath, respectively, which interact through

$$H_{SB} = \int dk \left(\sqrt{\frac{\gamma_p}{2\pi}} p_k^\dagger a_p + \sqrt{\frac{\gamma_s}{2\pi}} s_k^\dagger a_s \right) + \text{H.c.}, \quad (1)$$

where a_j is the system operator that couples to the signal or pump ($j = s/p$) bath.

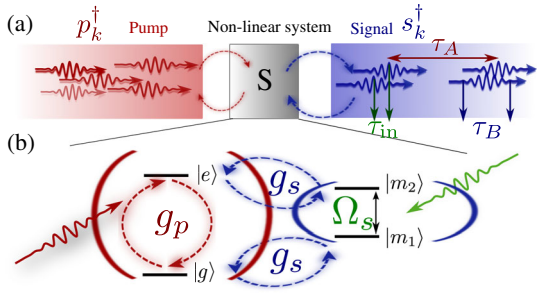

FIG. 1. Scheme for photon-pair generation. (a) The nonlinear system is driven through the pump bath (red) and the emission of photons coming out through the signal bath (blue) is analyzed. We depict the three relevant time scales that characterize the emission in our system: the intrinsic time scale of the single-photon wave packets (τ_B), and the separation between the pairs (τ_A) and between the photons within the same pair ($\tau_{\rm in}$). (b) Nonlinear system that provides the interface between incoming and outgoing photons.

We consider the cavity QED model depicted in Fig. 1(b) as the system S, which we have designed to deterministically convert single pump photons into signal photon pairs. It consists of a four-level system with states $\{|g\rangle, |m_1\rangle, |m_2\rangle, |e\rangle\}$, coupled to two photonic modes in independent cavities and a classical field. The *pump mode*, with annihilation operator a_p, is resonant with the $|g\rangle \leftrightarrow |e\rangle$ transition. The *signal mode*, on the other hand, has annihilation operator a_s and is resonant both with $|g\rangle \leftrightarrow |m_1\rangle$ and $|m_2\rangle \leftrightarrow |e\rangle$. Finally, the classical field controls resonantly the transition $|m_1\rangle \leftrightarrow |m_2\rangle$ with a Rabi frequency Ω_s, that will allow us to tune between different regimes of emission and, specifically, to induce deterministic down-conversion. In a picture rotating at the pump frequency, the system is then described by the Hamiltonian

$$H_S = g_p a_p^\dagger |g\rangle\langle e| + \Omega_s |m_2\rangle\langle m_1| + g_s a_s^\dagger (|m_2\rangle\langle e| + |g\rangle\langle m_1|) + \text{H.c.} \quad (2)$$

The scattering formalism [33] is naturally suited for analyzing processes such as the conversion of a given input state $|k_1, \ldots, k_m\rangle_p = p_{k_1}^\dagger \ldots p_{k_m}^\dagger |0\rangle$ with m incoming pump photons with momenta $\{k_1, \ldots, k_m\}$, into an outgoing state $|q_1, \ldots, q_n\rangle_s = s_{q_1}^\dagger \ldots s_{q_n}^\dagger |0\rangle$ with n signal photons with momenta $\{q_1, \ldots, q_n\}$. All the asymptotic information is contained in the so-called S matrix, defined as $S = \lim_{t_i \to -\infty}^{t_f \to +\infty} e^{iH_B t_f} e^{-iH(t_f - t_i)} e^{-iH_B t_i}$.

Let us study first the behavior of the system when excited by a single pump photon of momentum k_i, i.e., $|k_i\rangle_p$. In order for the photon to be perfectly down-converted to a signal photon pair, the condition ${}_p\langle k_f|S|k_i\rangle_p = 0 \; \forall \; k_f$ must be satisfied, that is, no photons are reflected in the pump bath. We show analytically in the Supplemental Material [34] that this condition can be satisfied under resonant excitation $k_i = 0$ for a specific control drive $\Omega_s = \Omega_{\rm 2ph}$ which reads

$$\Omega_{\rm 2ph}^2 \approx \gamma_s^2 [\Gamma_s(0) - \Gamma_p]/4\Gamma_p, \quad (3)$$

where we defined the Purcell-enhanced decay rates through the pump or signal cavities, $\Gamma_p = 4g_p^2/\gamma_p$ and $\Gamma_s(\Omega_s) = 4g_s^2\gamma_s/(\gamma_s^2 + 4\Omega_s^2)$, respectively, that we obtain by adiabatically eliminating the cavity modes and the intermediate levels [34]. Interestingly, $\Omega_{\rm 2ph}$ corresponds to the driving amplitude which makes these rates equal, i.e., $\Gamma_s(\Omega_{\rm 2ph}) = \Gamma_p$. This is a similar interference effect as the one used in previous works [38–43], which we exploit here to engineer perfect down-conversion even within the bad-cavity limit $g_j \ll \gamma_j$ $(j = p, s)$. Note that Eq. (3) requires $\Gamma_p < \Gamma_s(0) = 4g_s^2/\gamma_s$. Moreover, using scattering theory, we can show [34] that the *reflection coefficient* $|\int dk_p \langle k|S|k_i\rangle_p|^2$ has a Lorentzian shape as a function of the incident momentum k_i, with a width $\sim\Gamma_p + \Gamma_s(\Omega_s)$, which provides the bandwidth for efficient down-conversion of single-photon pulses.

To further characterize the down-conversion process, we calculate the outgoing two-photon wave function of the signal field, defined as $\Psi_{\rm 2ph}(x_1, x_2) = \langle 0|s(x_1)s(x_2)S|k_i\rangle_p$, with $s(x) = (2\pi)^{-1/2} \int dk s_k e^{ikx}$ annihilating signal excitations in real space. We provide its complete expression in [34], and here reproduce an approximate one in the bad-cavity limit and at resonance $k_i = 0$, which reads

$$|\Psi_{\rm 2ph}(x_1, x_2)|^2 \propto \left| e^{-\gamma_s \tau} - \frac{\gamma_s \sin(\Omega_s \tau)}{2\Omega_s} e^{-\Gamma_s(\Omega_s)\tau/2} \right|^2, \quad (4)$$

where $\tau = |x_1 - x_2|$. This expression shows that the wave function is indeed bunched, and therefore, the two output signal photons propagate together. Moreover, it is nonseparable, that is, the photons within the pair share entanglement. As shown in detail in [34], and following a similar route to that used in optical parametric down-conversion [44], we characterize this entanglement through the Schmidt number, which allows us to perform efficient analytical calculations by assuming the input wave packet to have a Lorentzian spectral shape. We provide quantitative details in [34], and here we just want to summarize our main numerical findings: (i) the entanglement shows a linear divergence with the inverse of the spectral width of the input wave packet, and (ii) for most of the parameters, the outgoing photons show strong nontrivial quantum correlations, becoming nonentangled only for $\Omega_s = 0$ and a specific width of the input wave packet. Note that this entanglement is different from the one of parametric sources such as those in [45], which are well described by Gaussian correlations between continuous variables.

An alternative scenario is that in which the system is continuously driven by a monochromatic laser at some

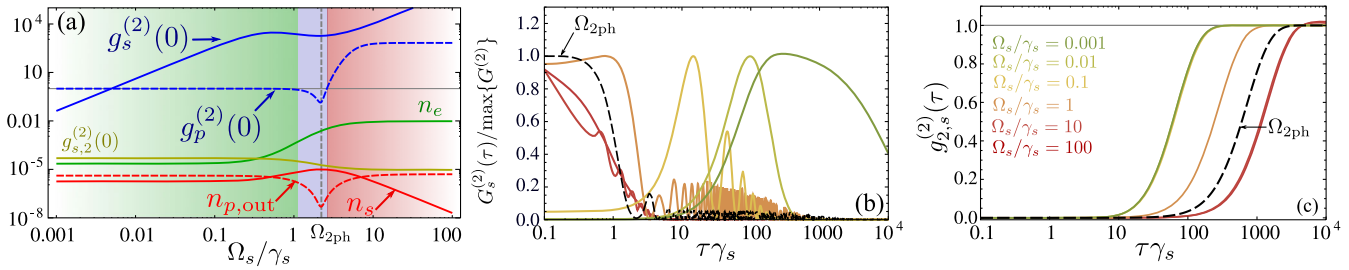

FIG. 2. (a) Main steady-state observables as a function of the control drive Ω_s. Parameters are $\gamma_p = 20\gamma_s$, $\Omega_p = 0.01\gamma_s$, $g_p = g_s = 0.1\gamma_s$. (b) and (c) show, respectively, $G_s^{(2)}(\tau)$ (or equivalently two-photon wave function) normalized to its maximal value and $g_{s,2}^{(2)}(\tau)$ (or equivalently four-photon wave function) as a function of τ for Ω_s changing logarithmically from $0.001\gamma_s$ to $100\gamma_s$ (in color) and for the optimal condition $\Omega_{2\mathrm{ph}}$ (dashed black) defined in Eq. (3). Notice that in (c) the curves from $\Omega_s = 10^{-3}$ to 0.1 and 10 to 100 overlap. We do not show the purity of two-photon emission [25] in the plots because, due to the way the system is engineered, it is 100% for all parameters.

frequency k_i through the pump bath (in the picture rotating with k_p). A standard approach in this context consists of integrating the bath degrees of freedom, which results in a master equation for the system's state ρ [46,47]:

$$\dot{\rho} = -i[H_S + H_D, \rho] + \sum_{j=s,p} \frac{\gamma_j}{2}(2a_j\rho a_j^\dagger - a_j^\dagger a_j\rho - \rho a_j^\dagger a_j), \tag{5}$$

where $H_D = \Omega_p(e^{-ik_i t}a_p^\dagger + \mathrm{H.c.})$ is a driving term, being Ω_p its amplitude (taken real and positive without loss of generality). The statistics of the field emitted through the baths can be analyzed through multitime correlation functions which, using input-output theory [46,47], can be related to system correlators $G_j^{(n)}(\tau_1, \ldots, \tau_n) = \langle a_j^\dagger(\tau_1)\ldots a_j^\dagger(\tau_n)a_j(\tau_n)\ldots a_j(\tau_1)\rangle$, where $\tau_1 < \ldots < \tau_n$ with the operators defined in the Heisenberg picture and $j = s$, p. The master equation allows evaluating these functions via the quantum regression theorem [46,47].

Even though scattering and master equation formalisms seem to apply to very different scenarios, they are very much connected [32,48,49]. For example, let us consider a situation in which H connects pump photons with signal photon pairs, which is the case of our system. Using the various definitions provided above, we find [34] a relation between scattering amplitudes and correlation functions of such a system under weak driving. In the case of the second-order correlation function, to first nontrivial order in Ω_p we get [34]

$$G_s^{(2)}(\tau) = \lim_{t\to\infty} G_s^{(2)}(t, t+\tau) \propto \Omega_p^2 |\Psi_{2\mathrm{ph}}(x_1, x_2)|^2. \tag{6}$$

We find a similar connection between the photon-pair second-order correlation function [25] and the four-photon wave function $\Psi_{4\mathrm{ph}}(x_1, x_2, x_3, x_4) = \langle 0|s(x_1)s(x_2)s(x_3)s(x_4)S|k_i, k_i\rangle_p$. This reads [34]

$$G_{s,2}^{(2)}(\tau) = \lim_{t\to\infty} G_s^{(4)}(t, t, t+\tau, t+\tau) \propto \Omega_p^4 |\Psi_{4\mathrm{ph}}(x_1, x_1, x_2, x_2)|^2. \tag{7}$$

Within the scattering formalism, it is clear that the system will be an ideal single photon-pair source whenever $|\Psi_{2\mathrm{ph}}(x_1, x_2)|$ has an absolute maximum around $x_1 = x_2$, while $|\Psi_{4\mathrm{ph}}(x_1, x_1, x_2, x_2)|$ shows a wide dip at that point, meaning that the system scatters photons in well-spaced wave packets containing two signal photons. Therefore, the equivalences above naturally give rise to a physical criterion characterizing when the weakly driven system is emitting light in photon pairs: $G_s^{(2)}(0) > G_s^{(2)}(\tau)$, while keeping $G_{s,2}^{(2)}(0) < G_{s,2}^{(2)}(\tau)$, that is, it has to show bunching of single photons, but antibunching between photon pairs. Moreover, the antibunching time scale must be larger than the bunching one, so that the separation between the pairs is guaranteed. This connection provides, then, formal grounds to the use in weakly driven systems of the photon-pair second-order correlation function [25].

Let us now analyze the behavior of our system under resonant continuous weak driving. In Fig. 2(a) we show the dependence of the main steady-state observables on the control drive Ω_s, as obtained from the master equation (5) or its connection with scattering theory [34], and using representative parameters within the bad-cavity limit. We represent various populations n_j ($j = p$ for pump, s for signal, and e for excited state), including the one for the output pump mode $a_{p,\mathrm{out}} = 2\Omega_p/\gamma_p - ia_p$, as well as normalized correlation functions $g_j^{(2)}(\tau) = G_j^{(2)}(\tau)/n_j^2$ and $g_{s,2}^{(2)}(\tau) = G_{s,2}^{(2)}(\tau)/[G_s^{(2)}(0)]^2$ at $\tau = 0$. We can differentiate three regimes of emission, best identified through the second-order correlation function of the pump. (i) $g_p^{(2)}(0) = 1$, green background: This region shows a transition from $g_s^{(2)}(0) < 1$, where the signal cavity is, therefore, emitting single photons, to $g_s^{(2)}(0) > 1$, which

corresponds to correlated emission from the cascade through the intermediate levels. However, when looking at the dynamics of $G_s^{(2)}(\tau)$ in Fig. 2(b), we can see how the maximum two-photon probability occurs at $\tau > 0$, and therefore it is still not a good photon-pair source, since this indicates that the photons inside the pair are spatially separated. (ii) $g_p^{(2)}(0) < 1$, blue background: This region shows $g_{s,2}^{(2)}(0) < g_{s,2}^{(2)}(\tau)$ as shown in Fig. 2(c), maximal $G_s^{(2)}(\tau)$ very close to $\tau = 0$, and a bunching time scale much shorter than the antibunching one of $g_{s,2}^{(2)}(\tau)$. Therefore, photons inside a pair are emitted together and the pairs are well separated, so the system behaves as a good photon-pair source according to the criterion defined above. Moreover, this region features a maximal signal population n_s (and minimal $n_{p,\mathrm{out}}$) at the optimum control drive $\Omega_{2\mathrm{ph}}$, yielding then a maximum photon-pair emission rate given by $\gamma_s n_s$. (iii) $g_p^{(2)}(0) > 1$, red background: With photon-pair emission but with a decrease of its rate.

In order to gain an understanding of the two-photon emission process, we analyze the relevant time scales for the emission of photon pairs, which are schematically depicted in Fig. 1(a), and we define in what follows. Once the system arrives at $|e\rangle$ it relaxes to $|g\rangle$ in a time τ_A (acting then as the *reloading* time), either emitting a pump photon or two cascaded signal photons separated by a time τ_{in}. Denoting by τ_B the intrinsic width of the single-photon wave packets, it is then clear that $\tau_{\mathrm{in}} < \tau_B < \tau_A$ is required for the system to act as an antibunched two-photon source. We have made a detailed analysis of these time scales [34], and here we focus on the results found within the bad-cavity limit ($g_j \ll \gamma_j$) and with a strong-enough control drive ($\Omega_s \gg g_j^2/\gamma_j$). In this regime, it is shown that τ_{in} scales as Ω_s^{-1}, and hence the delay between photons within the same pair can be made arbitrarily small by increasing the control drive. Under such circumstances, we get $\tau_B \sim \gamma_s^{-1}$, which determines the time scale of the bunching in $G_s^{(2)}(\tau)$, and provides the requirement $\Omega_s > \gamma_s$. Finally, τ_A is determined by the decay rate from $|e\rangle$ to $|g\rangle$ through the p and s channels, leading to $\tau_A^{-1} \approx \Gamma_p + \Gamma_s(\Omega_s)$. The different dependence of the scaling of these time scales with Ω_s explains the transition between the different regimes in Fig. 2.

To further estimate the feasibility of our proposal, we now analyze the effect of having spontaneous emission from $|e\rangle$ to $|g\rangle$ through other dissipative channels. Assuming such processes to occur at the rate $\gamma^* \ll \gamma_{p,s}$, this time scale contributes to the reloading time as $\tau_A^{-1} \approx \Gamma_s(\Omega_s) + \Gamma_p + \gamma^*$ [34]. It is then clear that as long as $\gamma^* \ll \gamma_s$, the condition $\tau_A \ll \{\tau_B, \tau_{\mathrm{in}}\}$ will then still be satisfied. Such an intuitive result is confirmed numerically [34], where we see that, as expected, by increasing γ^* above γ_s the system shows a transition from antibunched to bunched photon pairs, as τ_A becomes comparable to τ_B.

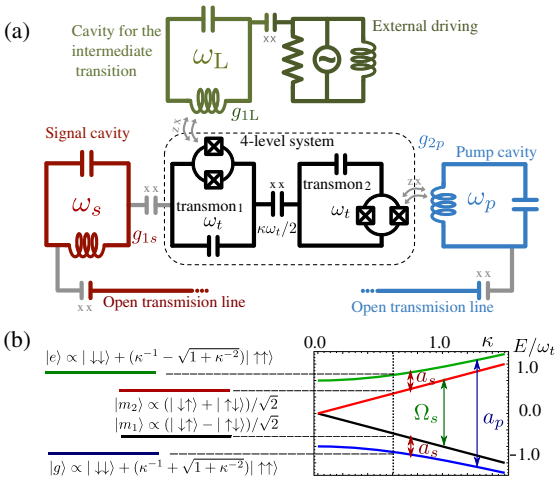

FIG. 3. (a) Circuit QED implementation: two coupled transmon qubits provide the desired four-level structure (b), while three LC circuits provide the single-mode cavities playing the role of signal, pump, and the classical driving for the intermediate transition. The baths are implemented with open transmission lines.

One versatile platform to implement our ideas is circuit QED [50–52], where we can use long-lived qubits, single-mode cavities, and open transmission lines to design our proposed setup. For concreteness, a specific architecture is depicted in Fig. 3(a), although it is important to note that any other architecture containing the ingredients and couplings that we introduce would work as well, as our ideas do not rely on the details of the implementation. Two identical qubits (transmons [53,54] in the figure, details can be found in [34]) with energies ω_t are capacitively coupled through an xx interaction $\omega_t \kappa \sigma_x^{(1)} \sigma_x^{(2)}/2$, whose spectrum is shown in Fig. 3(b). The desired four level structure appears between the states $|m_{2,1}\rangle \propto |\uparrow\downarrow\rangle \pm |\downarrow\uparrow\rangle$ and $|e,g\rangle \propto (\kappa^{-1} \mp \sqrt{1+\kappa^{-2}})|\uparrow\uparrow\rangle + |\downarrow\downarrow\rangle$, with respective energies $E_{2,1} = \pm\omega_t\kappa$ and $E_{e,g} = \pm\omega_t\sqrt{1+\kappa^2}$. Here, $|\downarrow\rangle$ and $|\uparrow\rangle$ are the ground and excited qubit states. Two single-mode LC resonators with frequencies $\omega_p = E_e - E_g$ and $\omega_s = E_e - E_2 = E_1 - E_g$ provide the pump and signal modes, respectively, while an additional strongly driven resonator with frequency $\omega_L = E_2 - E_1$ is used to control the intermediate transition. The pump and classical cavities are inductively coupled each to one transmon via xz interactions, $g_{2p}(a_p + a_p^\dagger)\sigma_z^{(2)}$ and $g_{1\mathrm{L}}(a_L + a_L^\dagger)\sigma_z^{(1)}$. Finally, the signal cavity is capacitively coupled through an xx interaction to one of the transmons, $g_{1s}(a_s + a_s^\dagger)\sigma_x^{(1)}$. Working in the $\kappa \ll 2$ regime and provided $\{g_{1\mathrm{L}}\alpha, g_{2p}\kappa, g_{1s}/\sqrt{2}\} \ll 2\omega_t\kappa$, these types of couplings ensure that in the eigenbasis of the two-qubit system the full system Hamiltonian takes the form of Eq. (2), with $\Omega_s = g_{1\mathrm{L}}\alpha$, $g_p = -g_{2p}\kappa$, and $g_s = g_{1s}/\sqrt{2}$ [34]—α being the number of excitations in the classical cavity that can be controlled via the external driving. Using $\gamma_{p,s}$ on the tens of MHz range, the spontaneous emission of the

superconducting qubits gets orders of magnitude below such large cavity decay rates, while the cooperativities $C_j = 4g_j^2/\gamma_j\gamma^*$ $(j = p,\ s)$ can be made very large since couplings g_{2p} and g_{1s} up to tens of MHz are routinely achieved in current experiments. With these parameters, at the optimal point $\Omega_s = \Omega_{2\mathrm{ph}}$, the rate of photon-pair emission $\gamma_s n_s$ can get up to the 0.1–10 kHz range for $\Omega_p/\gamma_s \in [10^{-2}, 10^{-1}]$.

Other platforms may fulfill our requisites in the optical domain, such as natural or artificial atoms using its "butterflylike" level structure, coupled to nanophotonic cavities. Current experiments with atoms [55] show cooperativities around 10, with decay rates up to 25 GHz, which would lead to photon-pair emission rates in the 0.1–10 MHz range, which already exceed current parametric down-conversion technologies.

Summing up, we have designed a cavity QED setup that acts as a deterministic down-converter when excited by single photons or as a continuous entangled photon-pair source when weakly driven, and does so within the bad-cavity limit. From the connection between the two regimes, we also formalized a criterion characterizing photon-pair sources under weak driving, based on the dynamics of the standard correlation function $g^{(2)}(\tau)$ and the generalized one of the pairs, $g_2^{(2)}(\tau)$, first introduced in [25]. Our analysis of the figures of merit and scaling with different parameters has shown the feasibility of the proposal, for which we have designed a concrete implementation based on superconducting circuits. We believe that our characterization, analysis, and implementation proposal represent an important step forward in the fabrication of efficient two-photon sources. We also foresee its extension to N-photon states, and, as a first step, we show in [34] how to obtain deterministic conversion of single photons into N photons, by using more elaborate schemes with $2N$ levels. We will analyze such setups in depth in future works.

We thank Peter Zoller, Eugenio Roldán, and J. Kofler for useful suggestions. We also appreciate the input of the anonymous referee, who encouraged us to characterize the entanglement properties of the photon pairs. This work has been funded by the European Union integrated project SIQS. A. G.-T. acknowledges support from the Intra-European Marie-Curie Fellowship NanoQuIS (625955). C. S. M. is supported by the FPI programme of the Spanish MINECO through Projects No. MAT2011- 22997 and No. MAT2014-53119-C2-1-R.

All the authors contributed equally to the project.

Note added.—Recently, a preprint appeared proposing an alternative route to deterministic down-conversion [43].

[1] B. Lounis and M. Orrit, Rep. Prog. Phys. **68**, 1129 (2005).
[2] J. L. O'Brien, Science **318**, 1567 (2007).
[3] J. L. O'Brien and J. V. Akira Furusawa, Nat. Photonics **3**, 687 (2009).
[4] C. Brunel, B. Lounis, P. Tamarat, and M. Orrit, Phys. Rev. Lett. **83**, 2722 (1999).
[5] R. J. Glauber, Phys. Rev. Lett. **10**, 84 (1963).
[6] I. Afek, O. Ambar, and Y. Silberberg, Science **328**, 879 (2010).
[7] V. Giovannetti, S. Lloyd, and L. Maccone, Phys. Rev. Lett. **96**, 010401 (2006).
[8] M. D'Angelo, M. V. Chekhova, and Y. Shih, Phys. Rev. Lett. **87**, 013602 (2001).
[9] W. Denk, J. Strickler, and W. Webb, Science **248**, 73 (1990).
[10] N. Horton, D. Wang, C. Kobat, F. Clark, C. Wise, and C. X. C. Schaffer, Nat. Photonics **7**, 205 (2013).
[11] N. Bruno, A. Martin, T. Guerreiro, B. Sanguinetti, and R. T. Thew, Opt. Express **22**, 17246 (2014).
[12] A. Ourjoumtsev, R. Tualle-Brouri, and P. Grangier, Phys. Rev. Lett. **96**, 213601 (2006).
[13] A. Zavatta, V. Parigi, and M. Bellini, Phys. Rev. A **78**, 033809 (2008).
[14] X.-C. Yao, T.-X. Wang, P. Xu, H. Lu, G.-S. Pan, X.-H. Bao, C.-Z. Peng, C.-Y. Lu, Y.-A. Chen, and J.-W. Pan, Nat. Photonics **6**, 225 (2012).
[15] C. K. Law and J. H. Eberly, Phys. Rev. Lett. **76**, 1055 (1996).
[16] G. Callsen, A. Carmele, G. Hönig, C. Kindel, J. Brunnmeier, M. R. Wagner, E. Stock, J. S. Reparaz, A. Schliwa, S. Reitzenstein, A. Knorr, A. Hoffmann, S. Kako, and Y. Arakawa, Phys. Rev. B **87**, 245314 (2013).
[17] A. Dousse, J. Suffczyński, A. Beveratos, O. Krebs, A. Lemaître, I. Sagnes, J. Bloch, P. Voisin, and P. Senellart, Nature (London) **466**, 217 (2010).
[18] M. Müller, S. Bounouar, K. D. Jöns, M. Glässl, and P. Michler, Nat. Photonics **8**, 224 (2014).
[19] M. Hofheinz, E. Weig, M. Ansmann, R. Bialczak, E. Lucero, M. Neeley, A. O'Connell, H. Wang, J. Martinis1, and A. Cleland, Nature (London) **454**, 310 (2008).
[20] M. Hofheinz, H. Wang, M. Ansmann, R. C. Bialczak, E. Lucero, M. Neeley, A. O'Connell, D. Sank, J. Wenner, J. M. Martinis *et al.*, Nature (London) **459**, 546 (2009).
[21] B. Johnson, M. Reed, A. Houck, D. Schuster, L. S. Bishop, E. Ginossar, J. Gambetta, L. DiCarlo, L. Frunzio, S. Girvin *et al.*, Nat. Phys. **6**, 663 (2010).
[22] D. Bozyigit, C. Lang, L. Steffen, J. M. Fink, C. Eichler, M. Baur, R. Bianchetti, P. J. Leek, S. Filipp, M. P. da Silva, A. Blais, and A. Wallraff, Nat. Phys. **7**, 154 (2011).
[23] C. Eichler, D. Bozyigit, C. Lang, L. Steffen, J. Fink, and A. Wallraff, Phys. Rev. Lett. **106**, 220503 (2011).
[24] M. Pechal, L. Huthmacher, C. Eichler, S. Zeytinoğlu, A. A. Abdumalikov, S. Berger, A. Wallraff, and S. Filipp, Phys. Rev. X **4**, 041010 (2014).
[25] C. Sanchez Muñoz, E. del Valle, A. G. Tudela, K. Müller, S. Lichtmannecker, M. Kaniber, C. Tejedor, J. Finley, and F. Laussy, Nat. Photonics **8**, 550 (2014).
[26] C. Sánchez-Muñoz, F. P. Laussy, C. Tejedor, and E. del Valle, New J. Phys. **17**, 123021 (2015).
[27] A. González-Tudela, V. Paulisch, D. E. Chang, H. J. Kimble, and J. I. Cirac, Phys. Rev. Lett. **115**, 163603 (2015).
[28] H.-G. Hong, H. Nha, J.-H. Lee, and K. An, Opt. Express **18**, 7092 (2010).

[29] M. Koch, C. Sames, M. Balbach, H. Chibani, A. Kubanek, K. Murr, T. Wilk, and G. Rempe, Phys. Rev. Lett. **107**, 023601 (2011).
[30] A. Rundquist, M. Bajcsy, A. Majumdar, T. Sarmiento, K. Fischer, K. G. Lagoudakis, S. Buckley, A. Y. Piggott, and J. Vučković, Phys. Rev. A **90**, 023846 (2014).
[31] A. Le Boité, G. Orso, and C. Ciuti, Phys. Rev. A **90**, 063821 (2014).
[32] T. Shi, D. E. Chang, and J. I. Cirac, Phys. Rev. A **92**, 053834 (2015).
[33] J. J. Sakurai and J. J. Napolitano, *Modern Quantum Mechanics* (Pearson Higher Ed., New York, 2014).
[34] See Supplemental Material at http://link.aps.org/supplemental/10.1103/PhysRevLett.117.203602 for details of the connection between scattering and master equation formalisms, the relevant time scales of the system, the entanglement of the outgoing photon pairs, and the proposed circuit QED architecture, which also contains Refs. [35–37].
[35] L. Zhou, Z. R. Gong, Y.-x. Liu, C. P. Sun, and F. Nori, Phys. Rev. Lett. **101**, 100501 (2008).
[36] J.-Q. Liao, H. K. Cheung, and C. K. Law, Phys. Rev. A **85**, 025803 (2012).
[37] N. Killoran, M. Cramer, and M. B. Plenio, Phys. Rev. Lett. **112**, 150501 (2014).
[38] K. Koshino, K. Inomata, T. Yamamoto, and Y. Nakamura, Phys. Rev. Lett. **111**, 153601 (2013).
[39] T. C. H. Liew and V. Savona, Phys. Rev. Lett. **104**, 183601 (2010).
[40] M. Bamba, A. Imamoğlu, I. Carusotto, and C. Ciuti, Phys. Rev. A **83**, 021802 (2011).
[41] A. Majumdar, M. Bajcsy, A. Rundquist, and J. Vučković, Phys. Rev. Lett. **108**, 183601 (2012).
[42] T. Shi and S. Fan, Phys. Rev. A **87**, 063818 (2013).
[43] E. Sánchez-Burillo, L. Martín-Moreno, J. García-Ripoll, and D. Zueco, arXiv:1602.05603.
[44] D. Horoshko, G. Patera, A. Gatti, and M. Kolobov, Eur. Phys. J. D **66**, 239 (2012).
[45] C. Eichler, D. Bozyigit, C. Lang, M. Baur, L. Steffen, J. M. Fink, S. Filipp, and A. Wallraff, Phys. Rev. Lett. **107**, 113601 (2011).
[46] G. W. Gardiner and P. Zoller, *Quantum Noise*, 2nd ed. (Springer-Verlag, Berlin, 2000).
[47] H. J. Carmichael, *Statistical Methods in Quantum Optics 1*, 2nd ed. (Springer, Berlin, 2002).
[48] T. Caneva, M. T. Manzoni, T. Shi, J. S. Douglas, J. I. Cirac, and D. E. Chang, New J. Phys. **17**, 113001 (2015).
[49] S. Xu and S. Fan, Phys. Rev. A **91**, 043845 (2015).
[50] Z.-L. Xiang, S. Ashhab, J. Q. You, and F. Nori, Rev. Mod. Phys. **85**, 623 (2013).
[51] M. Devoret and R. Schoelkopf, Science **339**, 1169 (2013).
[52] R. Schoelkopf and S. Girvin, Nature (London) **451**, 664 (2008).
[53] J. Koch, T. M. Yu, J. Gambetta, A. A. Houck, D. I. Schuster, J. Majer, A. Blais, M. H. Devoret, S. M. Girvin, and R. J. Schoelkopf, Phys. Rev. A **76**, 042319 (2007).
[54] J. A. Schreier, A. A. Houck, J. Koch, D. I. Schuster, B. R. Johnson, J. M. Chow, J. M. Gambetta, J. Majer, L. Frunzio, M. H. Devoret, S. M. Girvin, and R. J. Schoelkopf, Phys. Rev. B **77**, 180502 (2008).
[55] J. D. Thompson, T. G. Tiecke, N. P. de Leon, J. Feist, A. V. Akimov, M. Gullans, A. S. Zibrov, V. Vuletic, and M. D. Lukin, Science **340**, 1202 (2013).

Supplemental Material: Deterministic down-converter and continuous photon-pair source within the bad-cavity limit

Yue Chang,[1,*] Alejandro González-Tudela,[1,*] Carlos Sánchez Muñoz,[1,2,*] Carlos Navarrete-Benlloch,[1,3,*] and Tao Shi[1,*]

[1] *Max-Planck Institut für Quantenoptik, Hans-Kopfermann-Str. 1, D-85748 Garching, Germany*
[2] *Física Teórica de la Materia Condensada, Universidad Autónoma de Madrid, 28049 Madrid, Spain*
[3] *Institute for Theoretical Physics II, Universität Erlangen-Nürnberg, Staudtstrasse 7, 91058 Erlangen, Germany*

This supplemental material is divided in four main sections. The first one, Sec. SM1, is devoted to the scattering formalism. After introducing the S-matrix (Sec. SM1 A), we proceed to connect the multi-time correlation functions of a weakly-driven system with the scattering wave functions (Sec. SM1 B). We then explain how to compute scattering amplitudes (Sec. SM1 C) and wave functions (Sec. SM1 D) in an operationally simple manner, and apply those methods to our cavity QED model (Sec. SM1 E) proving that it can behave as a deterministic down-converter of entangled photon pairs (a property characterized in Sec. SM1 F), and providing an analytical analysis of the photon-pair emission timescales. In Sec. SM2 we provide an alternative formalism based on the master equation, which allows us to get insight into the properties of our cavity QED setup, including analytical expressions for its main observables. Sec. SM3 shows how our proposed circuit QED architecture provides an implementation of the model we are looking for. Sec. SM4 is the final one, which we use to show how our ideas for deterministic down-conversion can be extended to N-photon sources.

* All the authors contributed equally to the project.

SM1. SCATTERING THEORY RESULTS

A. Brief introduction to the S-matrix

The scattering formalism describes the asymptotic behaviour of free fields whose dynamics is governed by a Hamiltonian H_B, after having been scattered by some interacting Hamiltonian H. We use in particular the form of the Hamiltonian introduced in the main text

$$H = H_S + \underbrace{\int dk\, k(p_k^\dagger p_k + s_k^\dagger s_k)}_{H_B} + \underbrace{\int dk \left(\sqrt{\frac{\gamma_p}{2\pi}} p_k^\dagger a_p + \sqrt{\frac{\gamma_s}{2\pi}} s_k^\dagger a_s + \text{H.c.}\right)}_{H_{SB}}. \tag{SM1}$$

with a system Hamiltonian H_S independent of the bath operators (the fields), which interact with the system through H_{SB}.

Within the scattering formalism, all the asymptotic information can be extracted from the so-called S-matrix, defined by [1]

$$S = \lim_{\substack{t_f\to+\infty \\ t_i\to-\infty}} e^{iH_B t_f} e^{-iH(t_f-t_i)} e^{-iH_B t_i} = \lim_{t\to\infty} \mathcal{T}\left[e^{-i\int_{-t}^{t}\tilde{H}(t')dt'}\right], \tag{SM2}$$

where we have moved to the interaction picture, where the Hamiltonian is transformed into

$$\tilde{H}(t) = e^{iH_B t}(H_S + H_{SB})e^{-iH_B t} = H_S + \int dk \left(\sqrt{\frac{\gamma_p}{2\pi}} p_k^\dagger e^{ikt} a_p + \sqrt{\frac{\gamma_s}{2\pi}} s_k^\dagger e^{ikt} a_s + \text{H.c.}\right). \tag{SM3}$$

In addition, we have made use of the identity

$$\mathcal{T}\left[e^{-i\int_{t_0}^{t} dt' O(t')}\right] = e^{-iO_0 t}\mathcal{T}\left[\exp\left(-i\int_{t_0}^{t} dt' e^{iO_0 t'} O_1(t') e^{-iO_0 t'}\right)\right] e^{iO_0 t_0}, \tag{SM4}$$

valid for any operator $O(t) = O_0 + O_1(t)$, where $\mathcal{T}$ (time-ordering operator) orders Heisenberg-picture operators $A(t)$ and $B(t)$ as

$$\mathcal{T}[A(t_1)B(t_2)] = \begin{cases} A(t_1)B(t_2) & \text{if} \quad t_1 > t_2 \\ B(t_2)A(t_1) & \text{if} \quad t_1 < t_2 \end{cases}, \tag{SM5}$$

allowing to write the Dyson series in the compact form

$$\mathcal{T}\left[e^{-i\int_{t_0}^{t} dt' A(t')}\right] = 1 - i\int_{t_0}^{t} dt_1 A(t_1) - \int_{t_0}^{t} dt_1 \int_{t_0}^{t_1} dt_2 A(t_1)A(t_2) + i\int_{t_0}^{t} dt_1 \int_{t_0}^{t_1} dt_2 \int_{t_0}^{t_2} dt_3 A(t_1)A(t_2)A(t_3) + ... \tag{SM6}$$

B. Connection between the correlation functions and scattering wave functions

In this section we connect the wave functions which are naturally defined within the scattering formalism with correlation functions of the driven system, which are the objects naturally measured in quantum-optical experiments. Consider then the n-th correlation function of the field leaking out of the system through the signal bath, which can be written as [2, 3]

$$G_{\text{out}}^{(n)}(\tau_1, \tau_2, ..., \tau_n) = \langle 0 | s_{\text{out}}^\dagger(\tau_1) ... s_{\text{out}}^\dagger(\tau_n) s_{\text{out}}(\tau_n) ... s_{\text{out}}(\tau_1) | 0 \rangle \tag{SM7}$$

where $|0\rangle$ is the state with no excitations both in the system and the baths, we have assumed $\tau_1 < ... < \tau_n$, and defined the output field

$$s_{\text{out}}(\tau) = (2\pi)^{-1/2} \lim_{t\to\infty} \int dk\; s_k(t) e^{-ik(\tau - t)}, \tag{SM8}$$

with $s_k(t) = \mathcal{T}\left[e^{i\int_0^t dt'[H + H_D(t')]}\right] s_k \mathcal{T}\left[e^{-i\int_0^t dt'[H+H_D(t')]}\right]$ a bath operator in the Heisenberg picture, where we have included a driving term $H_D(t) = \Omega_p\left(e^{-ik_0 t} a_p^\dagger + \text{H.c.}\right)$ to the total Hamiltonian. Note that the well-known input-output relation [2, 3] $s_{\text{out}}(\tau) + s_{\text{in}}(\tau) = \sqrt{\gamma_s} a_s(\tau)$, with

$$s_{\text{in}}(\tau) = (2\pi)^{-1/2} \lim_{t\to 0} \int dk\; s_k(t) e^{-ik(\tau - t)}, \tag{SM9}$$

together with $[a_s(\tau), s_{\rm in}(\tau')] = 0$ for $\tau < \tau'$ (causality) and the fact that the signal bath is assumed to be in vacuum at the origin of times, allows connecting $G^{(n)}_{\rm out}$ with the correlation functions of system operators that we defined in the main text,

$$G^{(n)}_{\rm out}(\tau_1, \tau_2, ..., \tau_n) = \gamma_s^n \underbrace{\langle a_s^\dagger(\tau_1)...a_s^\dagger(\tau_n)a_s(\tau_n)...a_s(\tau_1)\rangle}_{G^{(n)}_s(\tau_1,\tau_2,...,\tau_n)}. \tag{SM10}$$

The correlation function can be written as

$$G^{(n)}_{\rm out}(\tau_1, \tau_2, ..., \tau_n) = \lim_{t\to\infty} {\rm tr}\left\{ s(x_n)...s(x_1)\mathcal{T}\left[e^{i\int_0^t dt'[H+H_D(t')]}\right]|0\rangle\langle 0|\,\mathcal{T}\left[e^{-i\int_0^t dt'[H+H_D(t')]}\right] s^\dagger(x_1)...s^\dagger(x_n)\right\}, \tag{SM11}$$

where $s(x) = (2\pi)^{-1/2}\int dk\, s_k e^{ikx}$ annihilates signal-field excitations in real space, and $x_n = t - \tau_n$. Let us now perform two unitary transformations inside the trace, which will allow us to easily get to the expression we are looking for. First, we apply $U = \exp(-iH_0 t)$ with $H_0 = \int dk\, k p_k^\dagger p_k$, which turns the correlation function into

$$G^{(n)}(\tau_1, \tau_2, ..., \tau_n) = \lim_{t\to\infty} {\rm tr}\left\{ s(x_n)...s(x_1)\mathcal{T}\left[e^{-i\int_0^t \tilde{H}(t')dt'}\right]|0\rangle\langle 0|\,\mathcal{T}\left[e^{i\int_0^t \tilde{H}(t')dt'}\right] s^\dagger(x_1)...s^\dagger(x_n)\right\}, \tag{SM12}$$

with

$$\tilde{H}(t) = U^\dagger(H+H_D)U - H_0 = H_S + \Omega_p\left(e^{-ik_0 t}a_p^\dagger + {\rm H.c.}\right) + \int dk\, k s_k^\dagger s_k + \int dk\left(\sqrt{\frac{\gamma_p}{2\pi}}p_k^\dagger e^{ikt}a_p + \sqrt{\frac{\gamma_s}{2\pi}}s_k^\dagger a_s + {\rm H.c.}\right), \tag{SM13}$$

where we have made use of (SM4). Let us now apply a displacement transformation D on mode k_0 of the pump bath, defined through $D^\dagger p_k D = p_k + \alpha_{k_0}\delta(k-k_0)$ with $\alpha_{k_0} = \sqrt{2\pi/\gamma_p}\Omega_p$, which making use of (SM4) again, turns the correlation function into

$$G^{(n)}_{\rm out}(\tau_1, \tau_2, ..., \tau_n) = \lim_{t\to\infty} {\rm tr}\left\{ s(x_n)...s(x_1)\mathcal{T}\left[e^{-i\int_0^t \bar{H}(t')dt'}\right]|\alpha_{k_0}\rangle\langle\alpha_{k_0}|\,\mathcal{T}\left[e^{i\int_0^t \bar{H}(t')dt'}\right] s^\dagger(x_1)...s^\dagger(x_n)\right\}, \tag{SM14}$$

where $|\alpha_{k_0}\rangle$ denotes the coherent state of the pump mode k_0, and

$$\bar{H}(t) = D^\dagger\tilde{H}D = H_S + \int dk\, k s_k^\dagger s_k + \int dk\left(\sqrt{\frac{\gamma_p}{2\pi}}p_k^\dagger e^{ikt}a_p + \sqrt{\frac{\gamma_s}{2\pi}}s_k^\dagger a_s + {\rm H.c.}\right). \tag{SM15}$$

Using now the expansion of the coherent states in the Fock basis, and undoing the U transformation, we obtain

$$G^{(n)}_{\rm out}(\tau_1, \tau_2, ..., \tau_n) = e^{-\alpha_{k_0}^2}\sum_{lm=0}^{\infty}\frac{\alpha_{k_0}^{m+l}}{\sqrt{l!m!}}\lim_{t\to\infty}\langle 0|\, p_{k_0}^m e^{iHt}s^\dagger(x_1)...s^\dagger(x_n)s(x_n)...s(x_1)e^{-iHt}p_{k_0}^{\dagger l}\,|0\rangle\,. \tag{SM16}$$

This expression is completely general, and its connection to scattering theory is not entirely clear, since the S-matrix is defined as $S = \lim_{\substack{t_f\to+\infty\\ t_i\to-\infty}} e^{iH_B t_f}e^{-iH(t_f-t_i)}e^{-iH_B t_i}$, while what appears on it is $\lim_{t\to\infty} e^{\pm iHt}$. Let us then particularize the expression to the case of interest for us, one in which the Hamiltonian H can only generate signal photons pair by pair from pump photons. Under such conditions, it is clear that the leading α_{k_0}-order in the previous expression is given by

$$G^{(n)}_{\rm out}(\tau_1, \tau_2, ..., \tau_n) = \frac{\alpha_{k_0}^{2\bar{m}}}{\bar{m}!}\lim_{t\to\infty}\left|\langle 0|\, s(x_n)...s(x_1)e^{-iHt}p_{k_0}^{\dagger\bar{m}}\,|0\rangle\right|^2, \tag{SM17}$$

where $\bar{m}$ is the minimum number of pump photons capable of generating n, that we assume to be an even number, signal photons, that is, $\bar{m} = n/2$. Now, it is also clear from the definition of the S-matrix that the matrix element in this expression and $\langle 0|\, s(x_n)...s(x_1)Sp_{k_0}^{\dagger\bar{m}}\,|0\rangle$ are equivalent up to a phase. Therefore, combining this expression with (SM10), we obtain the final result

$$G^{(n)}_s(\tau_1, \tau_2, ..., \tau_n) \propto \Omega_p^{2\bar{m}}\lim_{t\to\infty}|\langle 0|\, s(x_n)...s(x_1)Sp_{k_0}^{\dagger\bar{m}}\,|0\rangle|^2. \tag{SM18}$$

which particularized to to $n = 2$ and 4 coincide with the expressions provided in the main text. This expression connects the multi-time correlation functions of a weakly driven system with multi-photon wave functions obtained from the scattering theory, what we use in the main text to build a criterion characterizing when the system behaves as a proper single two-photon source.

C. Evaluation of scattering amplitudes

There exist severals methods to retrieve information from the S-matrix [4–8], but here we will use the method introduced in Ref. [6, 7], that we describe now. Within the scattering formalism one is naturally interested in how incoming pump-bath photons with well-defined momenta scatter into outgoing photons in the pump and signal baths (see Fig. 1 in the main text). The probabilities associated to such processes are encoded in the so-called *scattering amplitudes*, which are nothing but the S-matrix elements connecting the desired Fock states of the baths. For illustration, we calculate in detail the simplest among these proceses, namely the so-called *reflection amplitude*, which is the probability amplitude of a pump photon with momentum k_i to transform into an outgoing pump photon with momentum k_f. This is given by

$$ {}_p\langle k_f|S|k_i\rangle_p = \lim_{t\to\infty} \langle 0|p_{k_f} \mathcal{T}\left[e^{-i\int_{-t}^{t}\tilde{H}(t')dt'}\right] p^\dagger_{k_i}|0\rangle\,, \tag{SM19}$$

where we remind that $|0\rangle$ is the state with no excitations, that is, the common ground state of H_B and H_S. This expression depends on both bath and system operators, and our approach is designed to transform it in such a way that it can be evaluated simply from matrix elements of system operators. In order to do so, we proceed as follows. First, note that the previous expression can be written with the use of functional derivatives as

$$ {}_p\langle k_f|S|k_i\rangle_p = \lim_{t\to\infty} \frac{\delta}{\delta J^*_{k_f}}\frac{\delta}{\delta J_{k_i}} \langle 0|e^{\int dk J^*_k p_k}\mathcal{T}\left[e^{-i\int_{-t}^{t}\tilde{H}(t')dt'}\right] e^{\int dk J_k p^\dagger_k}|0\rangle\Big|_{\{J_k,J^*_k\}\to 0} \tag{SM20}$$

where $\{J_k, J^*_k\}$ are treated as independent classical currents for each bath mode, and we remind that the functional derivative acts as

$$ \frac{\delta}{\delta J_{k'}} J_k = \delta(k-k') \qquad \Longrightarrow \qquad \frac{\delta}{\delta J_{k'}} \exp\left(\int dk J_k A_k\right) = \exp\left(\int dk J_k A_k\right) A_{k'}, \tag{SM21}$$

valid for any operator A_k (and similarly for J^*_k). Introducing the displacement operator for the pump bath modes

$$ D(\{J_k\}) = \exp\left(\int dk J_k p^\dagger_k\right)\exp\left(\int dk J^*_k p_k\right)\exp\left(-\frac{1}{2}\int dk |J_k|^2\right) = \exp\left[\int dk \left(J_k p^\dagger_k - J^*_k p_k\right)\right], \tag{SM22}$$

which transforms the Hamiltonian as $\bar{H}(t) = D^\dagger(\{J_k\})\tilde{H}(t)D(\{J_k\}) = \tilde{H}(t) + H_D(t)$, that is, it adds a driving term

$$ H_D(t) = \int dk \sqrt{\frac{\gamma_p}{2\pi}}\left(J^*_k e^{ikt} a_p + J_k e^{-ikt} a^\dagger_p\right)\,, \tag{SM23}$$

we can rewrite Eq. (SM20) as

$$ {}_p\langle k_f|S|k_i\rangle_p = \lim_{t\to\infty} \frac{\delta}{\delta J^*_{k_f}}\frac{\delta}{\delta J_{k_i}} \langle 0|\mathcal{T}\left[e^{-i\int_{-t}^{t} dt_1 \bar{H}(t_1)}\right]|0\rangle e^{\int dk |J_k|^2}\Big|_{\{J_k,J^*_k\}\to 0}\,, \tag{SM24}$$

and then come back from the interaction picture to get

$$ {}_p\langle k_f|S|k_i\rangle_p = \lim_{t\to\infty} \frac{\delta}{\delta J^*_{k_f}}\frac{\delta}{\delta J_{k_i}} \langle 0|\mathcal{T}\left[e^{-i\int_{-t}^{t} dt_1 [H+H_D(t_1)]}\right]|0\rangle e^{\int dk |J_k|^2}\Big|_{\{J_k,J^*_k\}\to 0}\,. \tag{SM25}$$

Next we use the identity (SM4), together the Dyson series (SM6) for the remaining time-ordered exponential, and the Taylor series of the normalization factor $e^{\int dk|J_k|^2}$, so that acting with the functional derivatives we easily obtain

$$ {}_p\langle k_f|S|k_i\rangle_p = \delta(k_i-k_f) - \frac{\gamma_p}{2\pi}\int_{-\infty}^{\infty} dt_2 \int_{-\infty}^{\infty} dt_1 \langle 0|\mathcal{T}[a_p(t_2)a^\dagger_p(t_1)]|0\rangle e^{ik_f t_2 - ik_i t_1}, \tag{SM26}$$

where given a Schrödinger-picture operator A, we have defined the Heisenberg-picture operator $A(t) = e^{iHt}Ae^{-iHt}$. This equation can be further simplified by assuming that $|0\rangle$ is annihilated by the system operators a_j, so that we can write

$$ {}_p\langle k_f|S|k_i\rangle_p = \delta(k_i-k_f) - \frac{\gamma_p}{2\pi}\int_{-\infty}^{\infty} dt_2 \int_{-\infty}^{t_2} dt_1 \langle 0|a_p e^{iH(t_1-t_2)}a^\dagger_p|0\rangle e^{ik_f t_2 - ik_i t_1}. \tag{SM27}$$

We can rewrite this expression in terms of system operators only as follows:

$$ {}_p\langle k_f|S|k_i\rangle_p = \delta(k_i-k_f) - \frac{\gamma_p}{2\pi}\int_{-\infty}^{\infty} dt_2 \int_{-\infty}^{t_2} dt_1 \mathrm{tr}\left\{a_p e^{-iH(t_2-t_1)} a_p^\dagger |0\rangle\langle 0| e^{iH(t_2-t_1)}\right\} e^{ik_f t_2 - ik_i t_1} \tag{SM28a} $$

$$ = \delta(k_i-k_f) - \frac{\gamma_p}{2\pi}\int_{-\infty}^{\infty} dt_2 \int_{-\infty}^{t_2} dt_1 \mathrm{tr}_S\left\{a_p e^{\mathcal{L}(t_2-t_1)} a_p^\dagger |0\rangle_S\langle 0|\right\} e^{ik_f t_2 - ik_i t_1}\,, \tag{SM28b} $$

where in the second equality we have performed the trace over the bath as $\mathrm{tr}_B\{e^{-iH\tau}A_S e^{iH\tau}\} = e^{\mathcal{L}\tau}[A_S]$, valid for any system operator A_S, by defining the Liouville superoperator

$$ \mathcal{L}(\cdot) = -i[H_S^*(\cdot) - (\cdot)H_S^{*\dagger}] + \gamma_p a_p(\cdot)a_p^\dagger + \gamma_s a_s(\cdot)a_s^\dagger, \tag{SM29} $$

and the non-Hermitian system Hamiltonian

$$ H_S^* = H_S - i\frac{\gamma_p}{2}a_p^\dagger a_p - i\frac{\gamma_s}{2}a_s^\dagger a_s\,. \tag{SM30} $$

$|0\rangle_S$ is the ground state of H_S. In order to get to the final operationally-friendly expression, let us denote by $\tilde{A}$ a system operator evolved with the non-Hermitian Hamiltonian H_S^*, that is, $\tilde{A}(t) = e^{iH_S^* t}Ae^{-iH_S^* t}$. The presence of $|0\rangle_S$ in (SM28b), which we defined as ground state of H_S and assumed to be annihilated by the system operators a_j, prevents any contribution from the jumps induced by the last two terms of (SM29), so that (SM28b) can be rewritten as

$$ {}_p\langle k_f|S|k_i\rangle_p = \delta(k_i-k_f) - \frac{\gamma_p}{2\pi}\int_{-\infty}^{\infty} dt_2 \int_{-\infty}^{t_2} dt_1 \langle 0|\tilde{a}_p(t_2)e^{ik_f t_2}\tilde{a}_p^\dagger(t_1)e^{-ik_i t_1}|0\rangle \tag{SM31a} $$

$$ = \left(1 + i\gamma_p\langle 0|a_p\frac{1}{H_S^*-k_i}a_p^\dagger|0\rangle\right)\delta(k_i-k_f)\,. \tag{SM31b} $$

Note how this expression allows evaluating scattering amplitudes by simply inverting the system operator $H_S^* - k_i$.

The scattering amplitude manipulated above is important as it determines the reflection coefficient of single photons sent to the system through the pump bath. In our case, there are another two important scattering amplitudes related to the emission of signal photons. The first one corresponds to the probability amplitude of transforming an input pump photon with momentum k_i into two signal photons with momenta $\{q_1, q_2\}$, which following a similar approach as with the scattering amplitude above can be ultimately written as

$$ {}_s\langle q_1,q_2|S|k_i\rangle_p = i\sqrt{\frac{\gamma_p}{2\pi}}\frac{\gamma_s}{2\pi}\int_{\mathbb{R}^3} dt_1 dt_2 dt_3\; e^{i(q_1 t_3 + q_2 t_2 - k_i t_1)}\langle 0|\mathcal{T}\left[\tilde{a}_s(t_3)\tilde{a}_s(t_2)\tilde{a}_p^\dagger(t_1)\right]|0\rangle \tag{SM32a} $$

$$ = -i\gamma_s\sqrt{\frac{\gamma_p}{2\pi}}\;\langle 0|a_s\left[\frac{1}{H_S^*-q_1}+\frac{1}{H_S^*-q_2}\right]a_s\frac{1}{H_S^*-k_i}a_p^\dagger|0\rangle\;\;\delta(q_1+q_2-k_i)\,. \tag{SM32b} $$

Let us remark that the sum of two terms appearing inside the brackets appears because there are two different time-orderings which contribute, $\tilde{a}_s(t_3)\tilde{a}_s(t_2)\tilde{a}_p^\dagger(t_1)$ and $\tilde{a}_s(t_2)\tilde{a}_s(t_3)\tilde{a}_p^\dagger(t_1)$.

Similarly, the probability amplitude of transforming two input pump photons with momenta $\{k_1, k_2\}$ into four signal photons with momenta $\{q_1, q_2, q_3, q_4\}$ is given by a scattering amplitude which can written as

$$ {}_s\langle q_1,q_2,q_3,q_4|S|k_1,k_2\rangle_p = -\frac{\gamma_p}{2\pi}\left(\frac{\gamma_s}{2\pi}\right)^2\int_{\mathbb{R}^6}(\Pi_{i=1}^6 dt_i)e^{i(q_4 t_6 + iq_3 t_5 + q_2 t_4 + q_1 t_3 - k_2 t_2 - k_1 t_1)} \tag{SM33a} $$

$$ \times\langle 0|\mathcal{T}\left[\tilde{a}_s(t_6)\tilde{a}_s(t_5)\tilde{a}_s(t_4)\tilde{a}_s(t_3)\tilde{a}_p^\dagger(t_2)\tilde{a}_p^\dagger(t_1)\right]|0\rangle, $$

which can be trivially written in an operationally-friendly form similar to (SM31b) and (SM32b), but which is too lengthy to be written here since there many time-orderings which give nonzero contribution.

D. Evaluation of the two- and four-photon wave functions

The last two scattering amplitudes that we have given above, in Eqs. (SM32) and (SM33), are interesting because their Fourier transform provides the two- and four-photon wave functions introduced in the main text. Let us here provide closed expressions for these wave functions which can be evaluated directly from system operators.

In the case of the two-photon wave function, it is simple but lengthy by using (SM32a) to obtain

$$\Psi_{2\mathrm{ph}}(x_1,x_2)=\frac{1}{2\pi}\int dq_1\int dq_2\ {}_s\langle q_1,q_2|S|k_i\rangle_p e^{i(q_1x_1+q_2x_2)}=\sqrt{\frac{\gamma_p}{2\pi}}\gamma_s e^{ik_i\max\{x_1,x_2\}}\langle 0|a_s e^{-iH_S^*|x_1-x_2|}a_s\frac{1}{H_S^*-k_i}a_p^\dagger|0\rangle. \quad \text{(SM34)}$$

Note that, since the eigenvalues of H_S^* always have negative imaginary part, $\Psi_{2\mathrm{ph}}(x_1,x_2)\to 0$ when $|x_1-x_2|\to\infty$, showing that signal photons are emitted with a finite delay. From a practical point of view, this also means that this wave function has no independent scattering contribution. Therefore, in order to normalize it, e.g., one can divide by its maximal value in $|x_1-x_2|$ (or equivalently τ) as we did in Fig. 2(b) of the main text.

The four-photon wave function

$$\Psi_{4\mathrm{ph}}(x_1,x_2,x_3,x_4)=\frac{1}{(2\pi)^2}\int dq_1\int dq_2\int dq_3\int dq_4\ {}_s\langle q_1,q_2,q_3,q_4|S|k_1,k_2\rangle_p\ e^{i(q_1x_1+q_2x_2+q_3x_3+q_4x_4)} \quad \text{(SM35)}$$

can also be easily found, but is much more elaborate (and has a much lengthier final expression) in the general case. However, there are three relevant limits in which it is greatly simplified (we further assume $x_1>x_2>x_3>x_4$). First the limits $x_1-x_2\to\infty$ or $x_3-x_4\to\infty$, in which it vanishes identically, $\Psi_{4\mathrm{ph}}\to 0$, showing that the distance between the photons within the same pair is always finite, in agreement with what we found from the two-photon wave function. Second, the limit $x_2-x_3\to\infty$, which gives information about how the photons within the pairs behave when the system emits well-spaced pairs, and can be written as

$$\Psi_{4\mathrm{ph}}(x_1,x_2,x_3,x_4)=\Psi_{2\mathrm{ph}}(x_1,x_2)|_{k_i=k_1}\ \Psi_{2\mathrm{ph}}(x_3,x_4)|_{k_i=k_2}+\Psi_{2\mathrm{ph}}(x_1,x_2)|_{k_i=k_2}\ \Psi_{2\mathrm{ph}}(x_3,x_4)|_{k_i=k_1}\,, \quad \text{(SM36)}$$

which shows only independent scattering contributions where two incoming pump photons are scattered by the system independently into signal pairs described by the two-photon wave function (SM34). Thus, in this case we can normalize the general four-photon wave function to this independent scattering contribution, allowing us to compare directly with the normalized $g^{(2)}_{s,2}(\tau)$ shown in Fig. 2 (c) of the main text.

Finally, we consider the limit $x_1-x_2\to 0$ and $x_3-x_4\to 0$, which assumes the photons within the pairs to overlap perfectly and thus gives information about the relative distance $R=x_2-x_3$ between the the two-photon wave packets (describing then the bunching or antibunching between the photon pairs). We get $\Psi_{4\mathrm{ph}}(x_1,x_2,x_3,x_4)=\psi_{4\mathrm{ph}}(R;k_1,k_2)+\psi_{4\mathrm{ph}}(R;k_2,k_1)$, with

$$\psi_{4\mathrm{ph}}(R,k_1,k_2)=-\frac{\gamma_p}{2\pi}\gamma_s^2 e^{i(k_1+k_2)x_1}\left[\langle 0|a_s^2 e^{-iH_S^*R}a_s^2\frac{1}{k_1+k_2-H_S^*}a_p^\dagger\frac{1}{H_S^*-k_1}a_p^\dagger|0\rangle\right. \quad \text{(SM37)}$$
$$\left.+\langle 0|a_s^2\frac{e^{-iH_S^*R}-e^{-ik_2R}}{H_S^*-k_2}a_p^\dagger|0\rangle\langle 0|a_s^2\frac{1}{H_S^*-k_1}a_p^\dagger|0\rangle\right].$$

E. Application to our system Hamiltonian: condition for deterministic down-conversion and analysis of timescales

Let us now particularize the previous general results to our cavity QED system Hamiltonian, Eq. (5) in the main text, which we reproduce here for completeness

$$H_S=g_p\,a_p^\dagger|g\rangle\langle e|+\Omega_s|m_2\rangle\langle m_1|+g_s\,a_s^\dagger\,(|m_2\rangle\langle e|+|g\rangle\langle m_1|)+\mathrm{H.c.}\,, \quad \text{(SM38)}$$

where the states $\{|g\rangle,|m_1\rangle,|m_2\rangle,|e\rangle\}$ form a four-level system and a_j are bosonic annihilation operators associated to two cavity modes. It is important to note that the operator $C=2a_p^\dagger a_p+2|e\rangle\langle e|+a_s^\dagger a_s+|m_1\rangle\langle m_1|+|m_2\rangle\langle m_2|$ commutes with the Hamiltonian, and hence, H_S^* does not connect subspaces with different eigenvalue c of C. In particular, let us define the basis $\{|n\rangle_p\otimes|l\rangle_s\otimes|r\rangle=|n,l,r\rangle\}_{n,l=0,1,2,\ldots}^{r=g,m_1,m_2,e}$, where $|n\rangle_j$ is a Fock state for cavity mode j. Then the representation of H_S^* will have a box structure, each box corresponding to a subspace with well defined eigenvalue, e.g., $c=0$ spanned by $\{|0,0,g\rangle\}$, $c=1$ spanned by $\{|0,1,g\rangle,|0,0,m_1\rangle,|0,0,m_2\rangle\}$, $c=2$ spanned by $\{|1,0,g\rangle,|0,2,g\rangle,|0,0,e\rangle,|0,1,m_1\rangle,|0,1,m_2\rangle\}$, $c=3$ spanned by $\{|1,1,g\rangle,|0,3,g\rangle,|1,0,m_1\rangle,|1,0,m_2\rangle,|0,1,e\rangle,|0,2,m_1\rangle,|0,2,m_2\rangle\}$, or $c=4$ spanned by $\{|2,0,g\rangle,|1,2,g\rangle,|0,4,g\rangle,|0,2,e\rangle,|1,0,e\rangle,|0,3,m_1\rangle,|1,1,m_1\rangle,|1,1,m_2\rangle,|0,3,m_2\rangle\}$. In fact, these are all the subspaces that we need to consider in order to evaluate the main scattering amplitudes and wave functions introduced above.

For example, consider the reflection amplitude of an incoming pump photon, Eq. (SM31b); it is clear that this can be evaluated by considering the $c=2$ subspace of $H_S^*-i\gamma^*|e\rangle\langle e|/2$ (where we consider also spontaneous emission of

$|e\rangle$ to $|g\rangle$), which can be written as:

$$H_{S2}^{*}=\begin{pmatrix} -i\gamma_p/2 & 0 & g_p & 0 & 0 \\ 0 & -i\gamma_s & 0 & \sqrt{2}g_s & 0 \\ g_p & 0 & -i\gamma^*/2 & 0 & g_s \\ 0 & \sqrt{2}g_s & 0 & -i\gamma_s/2 & \Omega_s^* \\ 0 & 0 & g_s & \Omega_s & -i\gamma_s/2 \end{pmatrix}. \tag{SM39}$$

The reflection amplitude can be obtained then as

$${}_p\langle k_f|S|k_i\rangle_p=\left[1+i\gamma_p(H_{S2}^{*}-k_iI_{5\times5})_{11}^{-1}\right]\delta(k_i-k_f), \tag{SM40}$$

where $I_{5\times5}$ is the 5×5 identity matrix and $(H_{S2}^{*}-k_iI_{5\times5})_{11}^{-1}$ refers to element 11 of the inverse of the matrix $H_{S2}^{*}-k_iI_{5\times5}$, which can be easily found with the help of any symbolic program. Let us define the reflection coefficient $\mathcal{R}_p(k_i)=|1+i\gamma_p(H_{S2}^{*}-k_iI_{5\times5})_{11}^{-1}|^2$. Even though its full expression is too lengthy to be shown here, we have checked by exhaustive numerical inspection that within the bad-cavity limit it can be very well approximated by the Lorentzian

$$\mathcal{R}_p(k_i)=\left|1-\frac{2\Gamma_p}{\Gamma_p+\gamma^*+\Gamma_s(\Omega_s)-2ik_i}\right|^2, \tag{SM41}$$

where we have introduced the Purcell rates $\Gamma_p=4g_p^2/\gamma_p$ and $\Gamma_s(\Omega_s)=4g_s^2\gamma_s/(\gamma_s^2+4\Omega_s^2)$, and we have assumed $\gamma^*\ll\Gamma_p,\Gamma_s$. We see that deterministic down-conversion can be obtained only at resonance $k_i=0$ and by demanding ${}_p\langle k_f|S|k_i=0\rangle_p=0\ \ \forall k_f$, leading to an optimal control drive Ω_s given by

$$\Omega_{2\mathrm{ph}}^2=\frac{\gamma_s^2}{4}\frac{\Gamma_s(0)-(\Gamma_p-\gamma^*)}{\Gamma_p-\gamma^*}, \tag{SM42}$$

expression that coincides with the one given in the main text in limit of negligible spontaneous emission ($\gamma^*\to0$), Eq. (7), generalizing it to the case where spontaneous emission is present. Note that even in the presence of spontaneous emission it is still possible to obtain deterministic down-conversion, provided that certain conditions are satisfied. In particular, defining the cooperativites $C_j=4g_j^2/\gamma_j\gamma^*$, we see that assuming $C_p>1$ then the condition $C_s>C_p-1$ is required.

Proceeding in a similar way but making use of all the subspaces up to $c=4$, we can find analytical expressions for the two- and four-photon wave functions. These analytical expressions will allow us to see how the different timescales of photon-pair emission depend on the system parameters. For example, the two-photon wave function (SM34), it is easy to show that for resonant injection ($k_i=0$), and within the bad-cavity limit ($g_j\ll\gamma_j$) together with a strong control drive ($\Omega_s\gg g_s^2/\gamma_s$), we can write the corresponding probability as

$$|\Psi_{2\mathrm{ph}}(x_1,x_2)|^2\propto\left|2\Omega_s\exp[-(\gamma_s-\Gamma_s(\Omega_s))\,r/2]-\gamma_s\exp(-\Gamma_s(\Omega_s)r/2)\sin\left[\Omega_s\left(1+\frac{\Gamma_s(\Omega_s)}{2\gamma_s}\right)r\right]\right|^2, \tag{SM43}$$

where $r=|x_1-x_2|$. It is easy to find by numerical inspection that the value of r that maximizes this expression scales as Ω_s^{-1} for the regime of interest, i.e., $\Omega_s\gg\gamma_s(\gg\Gamma_s(0))$. This quantity is directly related to the timescale separation between the photons within the pair, denoted by τ_{in} in the main text, which we therefore find to scale as $\tau_{\mathrm{in}}\propto\Omega_s^{-1}$. Hence, the photons within the pair can be made to overlap very well simply by working with large Ω_s. On the other hand, under these circumstances the width of the two-photon wave function coincides with the intrinsic width of the emitted photons, denoted by τ_B in the main text, which for $\Omega_s\gg\gamma_s$ is simply given by the width of the first term in the expression above, that is, $\tau_B\approx\gamma_s^{-1}$. Thus, within the bad-cavity limit the $\Omega_s\gg\gamma_s$ condition ensures that the signal photon-pairs are emitted within the same temporal pulse (or spatial wave packet within the scattering formalism) since $\tau_{\mathrm{in}}\ll\tau_B$.

In order to study the separation or bunching between the photon pairs, what we called τ_A in the main text, we analyze the four-photon wave function $\Psi_{4\mathrm{ph}}(x_1,x_2,x_3,x_4)$ under the assumption that we satisfy the condition $\tau_{\mathrm{in}}\ll\tau_B$ as explained above. Under such conditions, we can fix $x_1-x_2\approx0$ and $x_3-x_4\approx0$, and use then expression (SM37) to study the four-photon wavefuntion at resonance ($k_1=k_2=0$). To get the timescale τ_A of antibunching between the pairs, we then need to study the dependence of (SM37) with the relative coordinate $R=x_2-x_3$ between the wave packets. Even though it is easy to find an analytic expression for it, it is too lengthy and nothing is gained from reproducing it here. However, in the bad-cavity limit it is possible to show that to second order in g_j/γ_j we get $|\psi_{4\mathrm{ph}}(R,k_1,k_2)|^2\propto|1-e^{-R/2\tau_A}|^2$, with

$$\tau_A^{-1}=\Gamma_s(\Omega_s)+\Gamma_p, \tag{SM44}$$

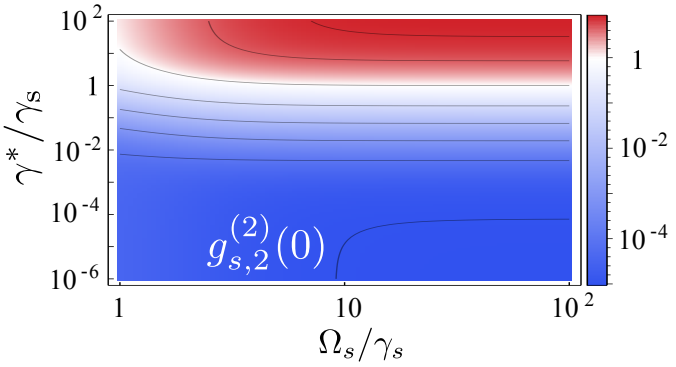

FIG. SM1. Density plot of the second-order correlation of the pairs at zero delay $g^{(2)}_{2,s}(0)$ as a function of Ω_s and γ^*, with the rest of parameters fixed as in Fig. 2 of the main text.

in the absence of spontaneous emission. This explains why in Fig. 2 (c), the curves with $\Omega_s \gg \gamma_s$ or $\Omega_s \ll \gamma_s$ collapse to a single antibunched curve with respective growth rates Γ_p or $\Gamma_p + \Gamma_s(0)$. When spontaneous emission is included this timescale must be modified. In particular, when $|\gamma_j - \gamma^*| \gg g_j$ is satisfied, we get

$$\tau_A^{-1} \approx \frac{2\left(\gamma_s - \gamma^*\right) g_s^2}{4\Omega_s^2 + \left(\gamma^* - \gamma_s\right)^2} + \frac{2g_p^2}{\gamma_p - \gamma^*} + \frac{\gamma^*}{2}\,, \tag{SM45}$$

which converges to the value provided in the main text when $\gamma^* \ll \gamma_j$. The results are also confirmed by the numerical simulation of Fig. SM1, where we show $g^{(2)}_{s,2}(0)$ as a function of the control driving Ω_s and γ^*, as obtained directly from numerical simulation of the master equation. As expected, by increasing γ^* above γ_s the system shows a transition from antibunched to bunched photon pairs, as τ_A becomes comparable to τ_B.

F. Entanglement properties of the photon-pair pulses

We proceed now to characterize the entanglement of the output signal photons. For this purpose, we analyze the situation in which input pump photon comes as a wave packet with finite bandwidth in k-space, that is, $|\Psi_{in}\rangle = \int_{-\infty}^{+\infty} dk w(k) p_k^\dagger |0\rangle$, with $\int_{-\infty}^{+\infty} dk |w(k)|^2 = 1$. From (SM32b), we see that the corresponding outgoing two-photon state can be written as

$$|\Psi_{2\mathrm{ph}}\rangle = \mathcal{N} \int_{\mathbb{R}^3} dk_\mathrm{p} dk_1 dk_2 w\left(k_p\right) \tilde{\Psi}_{2\mathrm{ph}}\left(k_\mathrm{p}, k_1, k_2\right) \delta\left(k_\mathrm{p} - k_1 - k_2\right)\ s_{k_1}^\dagger s_{k_2}^\dagger \left|0\right\rangle, \tag{SM46}$$

where $\mathcal{N}$ is a normalization constant and we have defined the (unnormalized) two-photon wave function in momentum space

$$\tilde{\Psi}_{2\mathrm{ph}}\left(k_\mathrm{p}, k_1, k_2\right) = \langle 0| a_s \frac{1}{H_\mathrm{S}^* - k_1} a_s \frac{1}{H_\mathrm{S}^* - k_\mathrm{p}} a_p^\dagger |0\rangle + \langle 0| a_s \frac{1}{H_\mathrm{S}^* - k_2} a_s \frac{1}{H_\mathrm{S}^* - k_\mathrm{p}} a_p^\dagger |0\rangle\,. \tag{SM47}$$

This state is very similar to that obtained in standard free-space optical parametric down-conversion, such that in order to analyze its entanglement we use the Schmidt number K as introduced in that context [9], which quantifies the number of correlated modes that that enter in the superposition of a given two-photon quantum state. The Schmidt number of a general bipartite system with subsystems A and B can be calculated as $K = 1/\mathrm{tr}\{\rho_A^2\}$, where ρ_A is the reduced density matrix of subsystem A. In our case, its evaluation is best performed by starting from the state written in coordinate space, that is,

$$|\Psi_{2\mathrm{ph}}\rangle = \mathcal{N} \int_{\mathbb{R}^2} dx_1 dx_2 F(x_1, x_2) s^\dagger(x_1) s^\dagger(x_2) \left|0\right\rangle, \tag{SM48}$$

where

$$F(x_1, x_2) = \int_{\mathbb{R}^2} \frac{dk_1 dk_2}{2\pi} e^{ik_1 x_1 + ik_2 x_2} w(k_1 + k_2) \tilde{\Psi}_{2\mathrm{ph}}(k_1 + k_2, k_1, k_2). \tag{SM49}$$

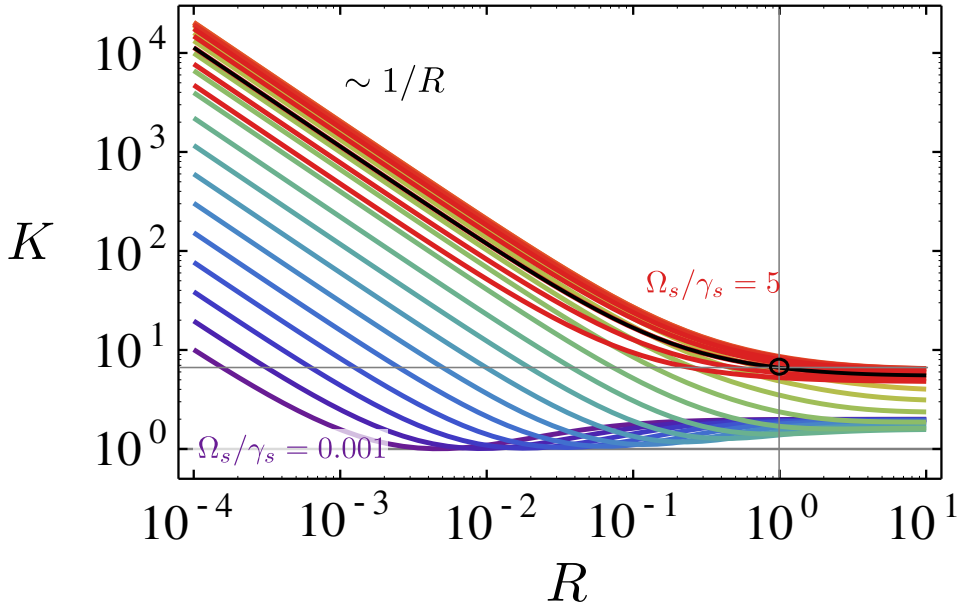

FIG. SM2. Schmidt number K as a function of the normalized width R of the input wave packet, for different values of the control drive Ω_s ranging from 0.01 (purple) to 5 (red). The rest of parameters are as in Fig. 2 of the main text. We have marked in black the curve corresponding to the optimal control drive $\Omega_s = \Omega_{2\mathrm{ph}}$, where our system behaves as a deterministic down-converter.

The Schmidt number can then be written as [9]

$$K^{-1} = \int_{\mathbb{R}^2} dx dx' |M(x,x')|^2 \,, \tag{SM50}$$

where $M(x,x')$ is defined as follows:

$$M\left(x,x'\right) = \frac{\int \mathrm{d}x_2 \; F\left(x,x_2\right) F^*\left(x',x_2\right)}{\int \mathrm{d}x_1 \mathrm{d}x_2 \left|F\left(x_1,x_2\right)\right|^2} \tag{SM51}$$

This expression requires the evaluation of several integrals whose complexity depends on the form of the wave packet $w(k)$. Since in our case the two-photon wave function can be written as a combination of exponentials with an argument linear in x_1 and x_2, see (SM43), a Lorentzian wave packet $w(k) = \sqrt{\Gamma_{\mathrm{in}}/\pi}(\Gamma_{\mathrm{in}} - ik)^{-1}$ with bandwidth Γ_{in} allows us to perform all the required integrals analytically, although the final expression is too lengthy to be written here. In Fig. SM2, for different values of the control drive Ω_s ranging from 0.001 to 5, we plot the Schmidt number K as a function of $R = \Gamma_{\mathrm{in}}/[\Gamma_p + \Gamma_s(\Omega_s)]$, that is the width of the input wave packet normalized to the characteristic emission rate of the system (SM44). The rest of parameters are as in Fig. 2 of the main text. Several things can be appreciated. First, note that for any Ω_s, the Schmidt number shows a linear divergence with R^{-1} as R goes to zero, that is, in the limit of plane-wave input (note the log-log plot); this divergence is characteristic of down-conversion processes, although the exact scaling depends on the shape of the input wave packet (for example, it is logarithmic for a Gaussian one in the case of optical free-space down-conversion [9]). Second, note that the state shows no correlations ($K = 1$) only for $\Omega_s \to 0$ and one specific width; in this limit, the two-photon state can be written as $b^{\dagger 2}|0\rangle$, where b is an annihilation operator that we will carefully characterize in future works. On the other hand, note that there are several instances in which the Schmidt number goes to 2 (for example $\Omega_s \to 0$ and $R \to \infty$); in those cases, the state can be written as $b_1^\dagger b_2^\dagger|0\rangle$, where $\{b_j\}_{j=1,2}$ are annihilation operators that we will study in the future, showing that the entanglement comes from the bosonic quantum statistics of the photonic modes, and not from the interaction. Note that it has been recently proposed a way of extracting this entanglement coming only from indistinguisability as a resource for quantum information purposes [10]. Finally, working at the optimal control drive $\Omega_s = \Omega_{2\mathrm{ph}}$ where the system behaves as a determinisitc down-converter for plane waves (black curve), the Schmidt number is always well above 2, showing that the outgoing photons are well entangled; for example, for a width matching the characteristic one of the system, $R = 1$, the Schmidt number is $K \approx 7$ (see the circled point).

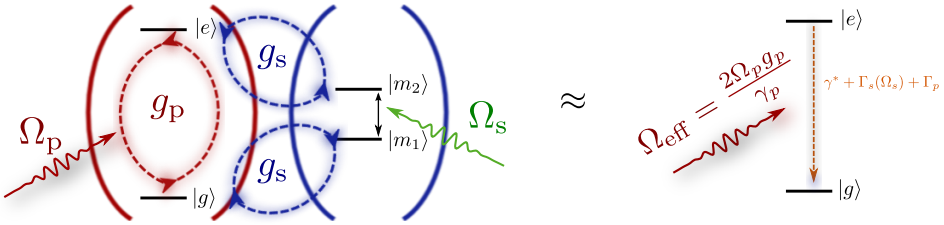

FIG. SM3. Effective two-level system resulting from the adiabatic elimination of all the degrees of freedom except for the ground and excited states. The effective system has an effective decay rate $\gamma_{\rm eff} = \Gamma_p + \Gamma_s(\Omega_s) + \gamma^*$ and effective coherent driving $\Omega_{\rm eff} = 2\Omega_p g_p/\gamma_p$.

SM2. EFFECTIVE CAVITY QED MODEL: EFFICIENCIES AND TIMESCALES.

This section aims at providing an intuitive understanding of our system by reducing it to a simpler one that allows explaining the underlying physics in an easier manner. In the previous section, we have shown how the interesting regime for the emission of photon pairs is the bad-cavity limit $g_j \ll \gamma_j$, together with $\Omega_s \gg \gamma_s$ such that photons are bunched. Under these conditions, the populations in the signal cavity and the intermediate levels $\{|m_1\rangle, |m_2\rangle\}$ are very small, while the population in the pump cavity is basically given by the driving laser, that is, $\langle a_p\rangle \approx 2\Omega_p/\gamma_p$. This allows for an adiabatic elimination of these degrees of freedom, such that the dynamics is captured by an effective two-level model defined by the states $\{|g\rangle, |e\rangle\}$, see Fig. SM3. In this reduced model, the coherent amplitude of the pump cavity acts as a driving term $\Omega_{\rm eff}(|g\rangle\langle e| + |e\rangle\langle g|)$ with $\Omega_{\rm eff} = 2\Omega_p g_p/\gamma_p$. In addition, there is an effective decay rate given by $\gamma_{\rm eff} = \Gamma_p + \Gamma_s(\Omega_s) + \gamma^*$, which is easily found by applying perturbation theory in the $c = 2$ subspace Hamiltonian (SM39). Note that this effective rate coincides with the reloading rate (SM44) that we found in the previous section.

The advantage of using this simplified model is two-fold: on the one hand it gives an intuitive and simplified picture of the dynamics of the system; moreover, due to the simplicity of the effective model, we can obtain analytical formulas from which reading the scaling of the relevant magnitudes, e.g, for the population of the signal cavity, n_s, which is related to the efficiency of two-photon emission. In order to obtain to obtain n_s, we will first obtain the population of the effective two level system $n_e = {\rm tr}\{\rho|e\rangle\langle e|\}$. In the simplified model n_e corresponds to the excited state population of a driven-dissipative two-level system, which is given by

$$n_e = \frac{4\Omega_{\rm eff}^2}{\gamma_{\rm eff}^2 + 8\Omega_{\rm eff}^2} = \frac{4g_p^2\Omega_p^2}{[\Gamma_p + \Gamma_s(\Omega_s) + \gamma^*]^2\gamma_p^2 + 8\Omega_p^2 g_p^2}\,, \tag{SM52}$$

The number N of transitions from $|e\rangle$ to $|g\rangle$ per unit time going through the signal cavity is given by $N = \Gamma_s(\Omega_s)n_e$, whereas the number of photons $N_{\rm s}$ emitted per unit time from the signal cavity is given by $N_{\rm s} = \gamma_{\rm s} n_s$. On the other hand, any time that one of the $|e\rangle \to |g\rangle$ transitions takes place through the signal cavity, two photons are emitted, and hence $N_{\rm s} = 2N$, leading to

$$n_s = 2\frac{\Gamma_s(\Omega_s)}{\gamma_{\rm s}} n_e \tag{SM53}$$

Maximizing this expression with respect to the control drive Ω_s, we obtain its optimal value. Interestingly, within the bad-cavity limit, this value coincides with the one obtained by demanding deterministic down-conversion in the scattering formalism, Eq. (SM42).

SM3. DETAILS ABOUT THE CIRCUIT QED IMPLEMENTATION

In this section we discuss in more depth show how our proposal could be implemented in circuit QED setups. For completeness and guidance in the presentation, we provide a simple concrete architecture presented in Fig. 3(a) of the main text, which we also reproduce here in Fig. SM5(a). However, it is important to note that any other architecture containing the ingredients and couplings that we require will work as well.

The four-level structure is obtained from two identical qubits coupled through an xx interaction, two capacitively-coupled transmons [11, 12] in Fig. SM5(a). For completeness, let us review here the physics behind a transmon

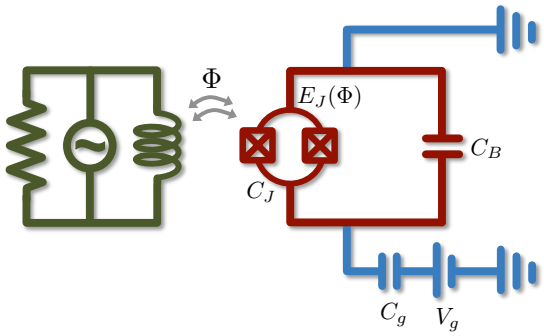

FIG. SM4. Simplified transmon circuit [11]. The basic circuit consists on a capacitor with capacitance C_B connected to two identical junctions in parallel (superconducting loop), which act as a single junction with capacitance C_J and nonlinear inductance $E_J(\Phi)$ tunnable through the magnetic flux generated by an external circuit. A gate voltage V_g is applied via a capacitor with capacitance C_g.

circuit, which is depicted in Fig. SM4. Using standard circuit-theory quantization, the Hamiltonian corresponding to this circuit can be written as [11]

$$H_{\text{transmon}} = 4E_C(N - n_g)^2 - E_J(\Phi)\cos(\varphi), \tag{SM54}$$

where $E_C = e^2/2(C_B + C_J + C_g)$ is the so-called charging energy (e is the electron charge), $E_J(\Phi) = \bar{E}_J|\cos(\Phi)|$ is the so-called Josephson energy associated to the superconducting loop, which can be tuned through an external bias magnetic flux Φ generated with another circuit, $\bar{E}_J$ is the bare Josephson energy associated to the junctions, and $n_g = C_g V_g/2e$ is related to the gate voltage bias. The aperators N and φ are, respectively, the number of cooper pairs transferred between between the superconductors which form the Josephson junctions and the phase difference between their macroscopic wave functions; they satisfy the commutation relation $[\varphi, N] = i/2\pi$. In the "charge" basis $\{|n\rangle\}_{n=0,1,2,\ldots}$ defined by $N|n\rangle = n|n\rangle$, the Hamiltonian is rewritten as

$$H_{\text{transmon}} = \sum_{n=0}^{\infty} 4E_C(n - n_g)^2|n\rangle\langle n| - \frac{E_J(\Phi)}{2}(|n\rangle\langle n+1| + |n+1\rangle\langle n|). \tag{SM55}$$

This Hamiltonian can be diagonalized analytically [11]. It turns out that close to the so-called "sweet spot" $n_g = 1/2$, the two lowest levels are well isolated from the rest, and made up only from the two lowest charge eigenstates, $|0\rangle$ and $|1\rangle$. Restricting the Hamiltonian to this subspace, and writing $n_g = \frac{1}{2} - \delta n_g$ with $|\delta n_g| \ll 1/2$, we get

$$H_{\text{transmon}} = 4E_c\delta n_g(|1\rangle\langle 1| - |0\rangle\langle 0|) - \frac{E_J(\Phi)}{2}(|0\rangle\langle 1| + |1\rangle\langle 0|), \tag{SM56}$$

where we have removed an $E_C(|1\rangle\langle 1| + |0\rangle\langle 0|)$ contribution, which acts as the identity on the restricted subspace we work on. At the sweet spot $\delta n_g = 0$, the transmon eigenstates become fair superpositions of the charge eigenstates, $|\uparrow\rangle = (|0\rangle - |1\rangle)/\sqrt{2}$ and $|\downarrow\rangle = (|0\rangle + |1\rangle)/\sqrt{2}$, with corresponding energies $E_{\uparrow,\downarrow} = \pm E_J(\Phi)/2$. Defining the Pauli matrices with respect these two states, for example, $\sigma_z = |\uparrow\rangle\langle\uparrow| - |\downarrow\rangle\langle\downarrow|$ and $\sigma_x = |\uparrow\rangle\langle\downarrow| + |\uparrow\rangle\langle\downarrow|$, the Hamiltonian is then rewritten as

$$H_{\text{transmon}} = \frac{E_J(\Phi)}{2}\sigma_z + 4E_c\delta n_g\sigma_x. \tag{SM57}$$

Furthermore, let us rewrite the external flux as $\Phi = \bar{\Phi} - \delta\Phi$, with $\bar{\Phi}$ around $\pi/4$ and $\delta\Phi \ll \bar{\Phi}$. We then Taylor-expand the Josephson energy around $\bar{\Phi}$ to first order in $\delta\Phi$, leading to

$$H_{\text{transmon}} = \frac{E_J(\bar{\Phi})}{2}\sigma_z + 4E_c\delta n_g\sigma_x + \frac{\bar{E}_J\sin(\bar{\Phi})}{2}\delta\Phi\sigma_z. \tag{SM58}$$

Hence, we finally get the Hamiltonian of a two-level system or qubit defined by the transmon eigenstates at the sweet spot, coupled capacitively through σ_x and inductively through σ_z to two weak external control fields.

Consider now two identical transmon qubits capacitively coupled as in Fig. SM5(a). Given the discussion above, and obviating the coupling to external weak fields, for such capacitive coupling the two-qubit Hamiltonian reads as

$$H_{\text{2qb}} = \frac{\omega_t}{2}\left(\sigma_z^{(1)} + \sigma_z^{(2)} + \kappa\sigma_x^{(1)}\sigma_x^{(2)}\right), \tag{SM59}$$

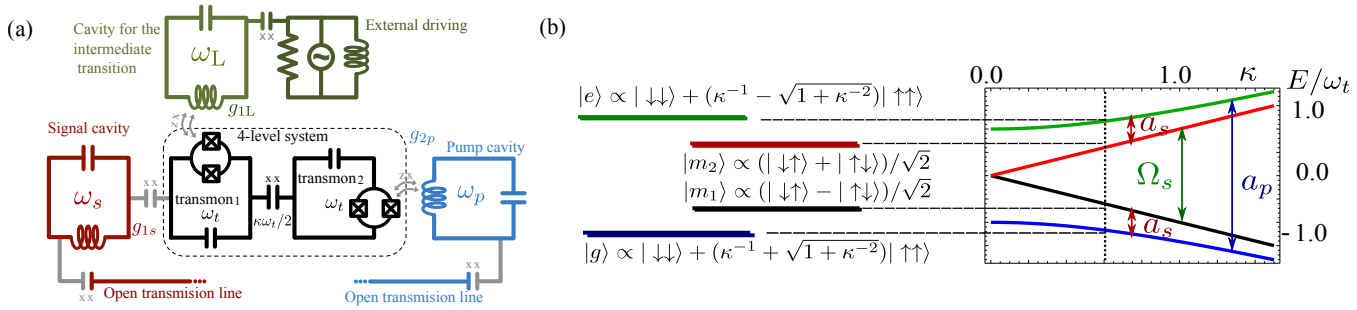

FIG. SM5. (a) Circuit QED implementation: two coupled transmon qubits provide the desired four-level structure (b), while three LC resonators provide the single-mode cavities playing the role of signal, pump, and the classical driving for the intermediate transition. The baths are implemented with open transmission lines.

where $\sigma_k^{(j)}$ is the k'th Pauli matrix associated to qubit j, and we have defined the qubit gap $\omega_t = E_J(\bar{\Phi})$, which have used to normalize the qubit coupling κ. The spectrum of this Hamiltonian is plotted in Fig. SM5(b), and it consists of the energies $E_{2,1} = \pm\omega_t\kappa$ corresponding to the symmetric and antisymmetric single-excited states $|m_{2,1}\rangle \propto |\uparrow\downarrow\rangle \pm |\downarrow\uparrow\rangle$, and the energies $E_{e,g} = \pm\omega_t\sqrt{1+\kappa^2}$ corresponding to the combinations $|e,g\rangle \propto (\kappa^{-1} \mp \sqrt{1+\kappa^{-2}})|\uparrow\uparrow\rangle + |\downarrow\downarrow\rangle$. Remarkably, the spectrum contains four levels with exactly the energy spacings that we require in our cavity QED proposal.

The next step consist on coupling the qubits to single-mode cavities in such a way that we reproduce the couplings that appear in the Hamiltonian H_S, Eq. (SM38), once everything is written in the two-qubit eigenbasis. There are several ways of accomplishing this. One possible way is depicted in Fig. SM5(a). We consider three LC resonators with characteristic frequencies ω_p (pump), ω_L ('laser'), and ω_s (signal). The pump and laser resonators are inductively coupled to qubits 2 and 1, respectively, while the signal resonator couples capacitively to the first qubit. The corresponding interaction Hamiltonians are easily found from the transmon theory that we reviewed above, and that lead to the Hamiltonian of Eq. (SM58): for capacitive coupling, one just needs to replace the static δn_g by an equivalent term coming from the voltage generated by the LC circuit, which is proportional to the x quadrature $a + a^\dagger$ of the circuit, where a is an annihilation operator; similarly, for an inductive coupling, one simply needs to replace the static flux $\delta\Phi$ by the magnetic flux induced by the current circulating in the LC circuit, which is again proportional to the corresponding x quadrature. Hence, capacitive couplings lead to an xx cavity-qubit interaction, while inductive couplings lead to an xz interaction. Therefore, the Hamiltonians coupling cavities and qubits in our system can be written as

$$H_{1L} = g_{1L}(a_L + a_L^\dagger)\sigma_z^{(1)} \approx g_{1L}(\alpha e^{-i\omega_L t} + \alpha^* e^{i\omega_L})\sigma_z^{(1)}\,, \tag{SM60a}$$
$$H_{2p} = g_{2p}(a_p + a_p^\dagger)\sigma_z^{(2)}\,, \tag{SM60b}$$
$$H_{1s} = g_{1s}(a_s + a_s^\dagger)\sigma_x^{(1)}\,, \tag{SM60c}$$

where a_j is the annihilation operator of the corresponding cavity, and in the first Hamiltonian we have assumed that the laser cavity is strongly driven, so that a_L can be replaced by its expectation value $\langle a_L\rangle = \alpha e^{-i\omega_L t}$.

We are going to show that, under certain conditions, these Hamiltonian terms provide the ones that we are looking for when written in the eigenbasis $\{|g\rangle, |m_1\rangle, |m_2\rangle, |e\rangle\}$ of the two-qubit system. To this aim, let us first remark that in such basis the single-qubit operators are written as

$$\sigma_z^{(1)} = |e\rangle\langle e| - |g\rangle\langle g| - \kappa|g\rangle\langle e| + |m_1\rangle\langle m_2| + \text{H.c.}, \tag{SM61a}$$
$$\sigma_z^{(2)} = |e\rangle\langle e| - |g\rangle\langle g| - \kappa|g\rangle\langle e| - |m_1\rangle\langle m_2| + \text{H.c.}, \tag{SM61b}$$
$$\sqrt{2}\sigma_x^{(1)} = |m_2\rangle\langle e| - |m_1\rangle\langle e| + |g\rangle\langle m_2| + |g\rangle\langle m_1| + \text{H.c.}, \tag{SM61c}$$

where, for the sake of simplifying the expressions, we have assumed $\kappa \ll 2$, though this is not really demanded for our system to work (the only requirement being that κ is not much bigger than 1 as this would make $|m_{1,2}\rangle$ and $|g,e\rangle$ nearly degenerate). Hence, in an interaction picture defined with respect to the free Hamiltonian $H_{2qb} + \omega_s a_s^\dagger a_s + \omega_p a_p^\dagger a_p$,

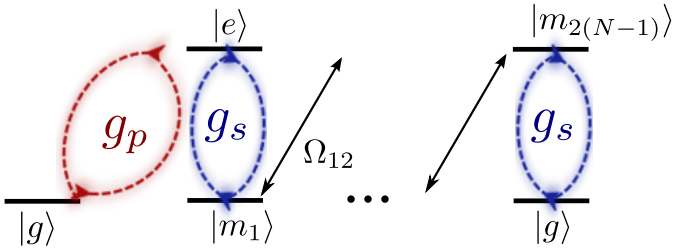

FIG. SM6. Level structure of the atom or artificial atoms system that allows us to generalize our results to N-photon sources. As before, the signal field is represented in blue, while the pump field is represented in red.

the coupling Hamiltonians (SM60) can be written as

$$H_{1\mathrm{L}}(t) = g_{1\mathrm{L}}\alpha^* e^{i\omega_{\mathrm{L}}t}\left(|e\rangle\langle e| - |g\rangle\langle g| - \kappa|g\rangle\langle e|e^{-2i\omega_t\sqrt{1+\kappa^2}t} + |m_1\rangle\langle m_2|e^{-2i\omega_t\kappa t} + \mathrm{H.c.}\right) + \mathrm{H.c.}, \tag{SM62a}$$

$$H_{2p}(t) = g_{2p}a_p^\dagger e^{i\omega_p t}\left(|e\rangle\langle e| - |g\rangle\langle g| - \kappa|g\rangle\langle e|e^{-2i\omega_t\sqrt{1+\kappa^2}t} - |m_1\rangle\langle m_2|e^{-2i\omega_t\kappa t} + \mathrm{H.c.}\right) + \mathrm{H.c.}, \tag{SM62b}$$

$$H_{1s}(t) = \frac{g_{1s}}{\sqrt{2}}a_s^\dagger e^{i\omega_s t}\Big[(|m_2\rangle\langle e| + |g\rangle\langle m_1|)e^{i\omega_t(\kappa-\sqrt{1+\kappa^2})t} + (|g\rangle\langle m_2| - |m_1\rangle\langle e|)e^{-i\omega_t(\kappa+\sqrt{1+\kappa^2})t} + \mathrm{H.c.}\Big] + \mathrm{H.c.}. \tag{SM62c}$$

We therefore see that choosing the frequencies of the LC resonators as $\omega_{\mathrm{L}} = 2\omega_t\kappa$, $\omega_p = 2\omega_t\sqrt{1+\kappa^2}$, $\omega_s = \omega_t(\sqrt{1+\kappa^2}-\kappa)$, we make resonant the couplings $\{\alpha|m_2\rangle\langle m_1|, a_p^\dagger|g\rangle\langle e|, a_s^\dagger(|m_2\rangle\langle e| + |g\rangle\langle m_1|)\}$ present in the target Hamiltonian (SM38), while the rest of the terms are suppressed within a rotating-wave approximation as long as $\{g_{1\mathrm{L}}\alpha, g_{2p}\kappa, g_{1s}/\sqrt{2}\} \ll 2\omega_t\kappa$. Under such conditions, we recover the desired Hamiltonian with the identifications $\Omega_s = g_{1\mathrm{L}}\alpha$, $g_p = -g_{2p}\kappa$, and $g_s = g_{1s}/\sqrt{2}$.

SM4. OUTLOOK: EXTENSION TO N-PHOTON STATES

In the main text, we focussed on how to achieve deterministic generation of photon pairs using an atomic 4-level structure. In these Section, we show how our ideas can be generalized to $N(>2)$-photon sources, by using more complicated level structures. We include here an initial analysis of the approximate wave functions and the deterministic conversion condition, leaving a more detailed analysis for a follow-up paper.

One way of generalizing our results to design N-photon sources is to use a level structure with $2N$ levels as sketched in Fig. SM6. Assuming that we move to a rotating frame where the hamiltonian in time-independent and that we consider all the processes to be resonant, the Hamiltonian describing the system reads:

$$\begin{aligned} H_S = {} & g_p\,|e\rangle\,\langle g|\,a_p + g_s\,|e\rangle\,\langle m_1|\,a_s + \Omega_{12}\,|m_1\rangle\,\langle m_2| + g_s\,|m_2\rangle\,\langle m_3|\,a_s + \Omega_{34}\,|m_3\rangle\,\langle m_4| + ... + \\ & g_s\,|m_{2N-4}\rangle\,\langle m_{2N-3}|\,a_s + \Omega_{2N-3,2N-2}\,|m_{2N-3}\rangle\,\langle m_{2N-2}| + g_s\,|m_{2N-2}\rangle\,\langle g|\,a_s + \mathrm{H.c.}, \end{aligned} \tag{SM63}$$

where $\Omega_{n,n+1}(n = 1, 3, ...2N-3)$ are the Rabi frequencies of the classical lasers connecting the $|e\rangle \to |g\rangle$ cascade. This Hamiltonian has to complemented with the corresponding Lindblad term associated to pump and signal cavity damping, at rates $\gamma_{s,p}$.

First, as we did for the $N = 2$ case, we calculate what is the reflection coefficient after the arrival of a single pump photon. Interestingly, assuming to work within the bad cavity limit, the reflection coefficient that governs the deterministic conversion condition is given, to lowest order in $g_{s,p}$, by

$${}_p\langle k_f|\,S\,|k_i\rangle_p \approx \left(\frac{2\Gamma_p}{\Gamma_p + \Gamma_s(\Omega_{12}) - 2ik_i} - 1\right)\delta(k_f - k_i), \tag{SM64}$$

where Γ_p and $\Gamma_s(\Omega_{12})$ are define as in the $N = 2$ case. As before, by tuning Ω_{12} such that $\Gamma_s(\Omega_{12}) = \Gamma_p$ we obtain the deterministic conversion condition at resonance k_i.

It is also instructive to obtain the N and $2N$ photon wave function, $\Psi_{\mathrm{Nph}}(x_1, ..., x_N) = \langle 0|s(x_1)...s(x_N)S|k_0\rangle_p$ and $\Psi_{2\mathrm{Nph}}(x_1, ..., x_N, x_{N+1}, ..., x_{2N}) = \langle 0|s(x_1)...s(x_{2N})S|k_0, k_0\rangle_p$, under the deterministic conversion condition. As before, their general expressions are very lengthy; however, using the intuition that we gained from the $N = 2$ situation, simplified expressions are expected by working in the regime where $\Omega_{n,n+1}$ and $|\Omega_{n,n+1} - \Omega_{n+2,n+3}|$ are much larger than γ_s. Indeed, under these conditions the N-photon wave function takes the simple approximate form

$$\Psi_{\mathrm{Nph}}(x_1, x_2, ..., x_N) \propto e^{-\gamma_s(x_{N-1}-x_N)/2}e^{-\gamma_s(x_{N-2}-x_{N-1})}...e^{-(N-2)\gamma_s(x_2-x_3)/2}e^{-(N-1)\gamma_s(x_1-x_2)/2}, \tag{SM65}$$

which is bunched and entangled as in the $N = 2$ case. Similarly, the $2N$-photon wave function can be approximated to the second order in $g_{p,s}$ as

$$\Psi_{2\mathrm{Nph}}(x_1, ..., x_1, x_1 - \tau, ..., x_1 - \tau) \propto 1 - e^{-[\Gamma_s(\Omega_{12})+\Gamma_p]\tau/2}\,, \tag{SM66}$$

which is therefore antibunched with the same timescale as in the $N = 2$ case.

These results show that our deterministic down conversion mechanism can indeed be extended for the generation of N-photon states.

[1] J. J. Sakurai and J. J. Napolitano, *Modern quantum mechanics* (Pearson Higher Ed, 2014).
[2] G. W. Gardiner and P. Zoller, *Quantum Noise*, 2nd ed. (Springer-Verlag, Berlin, 2000).
[3] H. J. Carmichael, *Statistical methods in quantum optics 1*, 2nd ed. (Springer, 2002).
[4] L. Zhou, Z. R. Gong, Y.-x. Liu, C. P. Sun, and F. Nori, Phys. Rev. Lett. **101**, 100501 (2008).
[5] J.-Q. Liao, H. K. Cheung, and C. K. Law, Phys. Rev. A **85**, 025803 (2012).
[6] T. Caneva, M. T. Manzoni, T. Shi, J. S. Douglas, J. I. Cirac, and D. E. Chang, New Journal of Physics **17**, 113001 (2015).
[7] T. Shi, D. E. Chang, and J. I. Cirac, Phys. Rev. A **92**, 053834 (2015).
[8] S. Xu and S. Fan, Physical Review A **91**, 043845 (2015).
[9] D. Horoshko, G. Patera, A. Gatti, and M. Kolobov, Eur. Phys. J. D **66**, 239 (2012).
[10] N. Killoran, M. Cramer, and M. B. Plenio, Phys. Rev. Lett. **112**, 150501 (2014).
[11] J. Koch, T. M. Yu, J. Gambetta, A. A. Houck, D. I. Schuster, J. Majer, A. Blais, M. H. Devoret, S. M. Girvin, and R. J. Schoelkopf, Phys. Rev. A **76**, 042319 (2007).
[12] J. A. Schreier, A. A. Houck, J. Koch, D. I. Schuster, B. R. Johnson, J. M. Chow, J. M. Gambetta, J. Majer, L. Frunzio, M. H. Devoret, S. M. Girvin, and R. J. Schoelkopf, Phys. Rev. B **77**, 180502 (2008).